Decision Support System for Automatic Identification of ROI (Region of Interest) for Medical Images

A Thesis submitted to Gujarat Technological University

for the Award of

Doctor of Philosophy

in

COMPUTER SCIENCE

by

RUTVI RUSHABH SHAH
Enrollment No: 129990931004

under supervision of

Dr. PRIYANKA SHARMA

GUJARAT TECHNOLOGICAL UNIVERSITY
AHMEDABAD

April – 2018

Decision Support System for Automatic Identification of ROI (Region of Interest) for Medical Images

A Thesis submitted to Gujarat Technological University

for the Award of

Doctor of Philosophy

in

COMPUTER SCIENCE

by

RUTVI RUSHABH SHAH
Enrollment No: 129990931004

under supervision of

Dr. PRIYANKA SHARMA

GUJARAT TECHNOLOGICAL UNIVERSITY
AHMEDABAD

April – 2018

DECLARATION

I declare that the thesis entitled **Decision Support System for Automatic Identification of ROI (Region of Interest) for Medical Images** submitted by me for the degree of Doctor of Philosophy is the record of research work carried out by me during the period from July 2013 to June 2017 under the supervision of Dr. Priyanka Sharma and this has not formed the basis for the award of any degree, diploma, associateship, fellowship, titles in this or any other University or other institution of higher learning.

I further declare that the material obtained from other sources has been duly acknowledged in the thesis. I shall be solely responsible for any plagiarism or other irregularities, if noticed in the thesis.

Signature of the Research Scholar:…… Date: …./……/……

Name of Research Scholar: Rutvi Rushabh Shah

Place: Ahmedabad

CERTIFICATE

I certify that the work incorporated in the thesis **Decision Support System for Automatic Identification of ROI (Region of Interest) for Medical Images** submitted by Smt. **Rutvi Rushabh Shah** was carried out by the candidate under my supervision/guidance. To the best of my knowledge: (i) the candidate has not submitted the same research work to any other institution for any degree/diploma, Associateship, Fellowship or other similar titles (ii) the thesis submitted is a record of original research work done by the Research Scholar during the period of study under my supervision, and (iii) the thesis represents independent research work on the part of the Research Scholar.

Signature of Supervisor: ……..…… Date: …./……/……

Name of Supervisor: Dr. Priyanka Sharma

Place: Ahmedabad

Originality Report Certificate

It is certified that Ph.D. Thesis titled **Decision Support System for Automatic Identification of ROI (Region of Interest) for Medical Images** by **Rutvi Rushabh Shah** has been examined by us. We undertake the following:

a. Thesis has significant new work / knowledge as compared already published or are under consideration to be published elsewhere. No sentence, equation, diagram, table, paragraph or section has been copied verbatim from previous work unless it is placed under quotation marks and duly referenced.

b. The work presented is original and own work of the author (i.e. there is no plagiarism). No ideas, processes, results or words of others have been presented as Author own work.

c. There is no fabrication of data or results which have been compiled/analyzed.

d. There is no falsification by manipulating research materials, equipment or processes, or changing or omitting data or results such that the research is not accurately represented in the research record.

e. The thesis has been checked using **Turnitin** (copy of originality report attached) and found within limits as per GTU Plagiarism Policy and instructions issued from time to time (i.e. permitted similarity index <=25%).

Signature of the Research Scholar:…… Date: …./……/……

Name of Research Scholar: Rutvi Rushabh Shah

Place: Ahmedabad

Signature of Supervisor: …… Date: …./……/……

Name of Supervisor: Dr. Priyanka Sharma

Place: AHMEDABAD

Decision Support System for Automatic Identification of Region of Interest in Medical Images

ORIGINALITY REPORT

%18	%14	%11	%12
SIMILARITY INDEX	INTERNET SOURCES	PUBLICATIONS	STUDENT PAPERS

PRIMARY SOURCES

1	www.sersc.org Internet Source	%1
2	uu.diva-portal.org Internet Source	%1
3	ijarcsse.com Internet Source	%1
4	Jie Wu, Yang Tang, Pavani Davuluri, Kevin R. Ward, Ashwin Belle, Rosalyn S. Hobson,	%1


turnitin
18%
SIMILAR
--
OUT OF 0
Match Overview
1
www.sersc.org
Internet source
1%
2
uu.diva-portal.org
Internet source
1%
3
ijarcsse.com
Internet source
1%
4
Jie Wu. "Fracture detec...
Publication
1%
5
elib.dlr.de
Internet source
1%
6
www.ijetae.com
Internet source
1%
7
"Emmy for Marconi", El...
Publication
<1%

PhD THESIS Non-Exclusive License to GUJARAT TECHNOLOGICAL UNIVERSITY

In consideration of being a PhD Research Scholar at GTU and in the interests of the facilitation of research at GTU and elsewhere, I, **Rutvi Rushabh Shah** having Enrollment No. 129990931004 hereby grant a non-exclusive, royalty-free and perpetual license to GTU on the following terms:

a) GTU is permitted to archive, reproduce and distribute my thesis, in whole or in part, and/or my abstract, in whole or in part (referred to collectively as the "Work") anywhere in the world, for non-commercial purposes, in all forms of media;

b) GTU is permitted to authorize, sub-lease, sub-contract or procure any of the acts mentioned in paragraph (a);

c) GTU is authorized to submit the Work at any National / International Library, under the authority of their "Thesis Non-Exclusive License";

d) The Universal Copyright Notice (©) shall appear on all copies made under the authority of this license;

e) I undertake to submit my thesis, through my University, to any Library and Archives. Any abstract submitted with the thesis will be considered to form part of the thesis.

f) I represent that my thesis is my original work, does not infringe any rights of others, including privacy rights, and that I have the right to make the grant conferred by this non-exclusive license.

g) If third party copyrighted material was included in my thesis for which, under the terms of the Copyright Act, written permission from the copyright owners is required, I have obtained such permission from the copyright owners to do the acts mentioned in paragraph (a) above for the full term of copyright protection.

h) I retain copyright ownership and moral rights in my thesis and may deal with the copyright in my thesis, in any way consistent with rights granted by me to my University in this non-exclusive license.

i) I further promise to inform any person to whom I may hereafter assign or license my copyright in my thesis of the rights granted by me to my University in this non-exclusive license.

j) I am aware of and agree to accept the conditions and regulations of PhD including all policy matters related to authorship and plagiarism.

Signature of the Research Scholar: _____

Name of Research Scholar: Rutvi Rushabh Shah

Date: _____ Place: Ahmedabad

Signature of Supervisor: _____

Name of Supervisor: Dr. Priyanka Sharma

Date: _____ Place: Ahmedabad

Seal:

Thesis Approval Form

The viva-voce of the PhD Thesis submitted by **Smt. Rutvi Rushabh Shah** (Enrollment No. 129990931004) entitled **Decision Support System for Automatic Identification of ROI (Region of Interest) for Medical Images** was conducted on _____(day and date) at Gujarat Technological University.

(Please tick any one of the following options)

☐ The performance of the candidate was satisfactory. We recommend that he/she be awarded the PhD degree.

☐ Any further modifications in research work recommended by the panel after 3 months from the date of first viva-voce upon request of the Supervisor or request of Independent Research Scholar after which viva-voce can be re-conducted by the same panel again.

(briefly specify the modifications suggested by the panel)

☐ The performance of the candidate was unsatisfactory. We recommend that he/she should not be awarded the PhD degree.

(The panel must give justifications for rejecting the research work)

Name and Signature of Supervisor with Seal

---

1) (External Examiner 1) Name and Signature

---

2) (External Examiner 2) Name and Signature

---

3) (External Examiner 3) Name and Signature

ABSTRACT

Today bone fractures are very common in our country because of road accidents, sports injuries and falls. Patients with bone fractures who go into shock state have a mortality of 30-50%. When combined with other injuries in the body, for example, an abdominal injury, the chance of mortality rises even higher, approaching 100% in some cases.

According to the market report of India Today, the fracture features more in Indian hospital records and the incidences have increased 3-folds over the past 3 decades with more than 4.4 lakh people and is expected to increase to more than 6 lakh in 2020.

The X-Ray images are the most common means of medical imaging accessibility for people during the injuries and accidents. X-rays are the oldest and most frequent form of medical imaging. But the minute fracture detection in the X-Ray image is not possible due to the complexity of bone structure and the difference in visual characteristics of fracture by their location. So it is difficult to accurately detect and locate the fractures and also determine the severity of the injury. The major challenges of X-Ray imaging are the presence of noise, intensity ambiguity, and overlapping tissues. This creates a hurdle in correct diagnosis and delays treatment. The numerous incidences necessitate the health care professionals to analyze a huge number of x-ray images. The use of computer-assisted automatic detection of fractures in X-Ray images can be a significant contribution for assisting the physicians in making faster and more accurate diagnostic decisions and fasten treatment planning.

Among fractures, automatic detection is considered more challenging because they are different and variable in presentation and their outcomes are unpredictable. The major challenges for computer-assisted automated fracture detection can be accurate segmentation process, automatic identification of the region of interest (bone fracture), evaluation and suggestive course of action.

The research proposes an automatic algorithm (ROIMI) for detecting bone fracture in the X-Ray image. The proposed algorithm processes image step by step to obtain the results. The first step is segmentation. Segmentation facilitates the process partitioning bone for faster and better identification of the region of interest (ROI) from the X-ray image. The

next step is to identify the region of interest. The region of interest (bone fracture) is a diagnostically important part of the analysis and suggesting the type of fracture based on its size.

The simulation results obtained by running the algorithm on X-ray images of different fractures types show a recall of more than 80%. The results are promising, demonstrating that the proposed algorithm is fairly accurate and capable of automatically identifying and classifying hairline, minor and major types of fractures and shows potential for clinical application. The use of this novel algorithm shows that it can help to minimize the diagnostic errors and fasten the process of healthcare by providing an accurate and fully automated system for identification of fractures and suggesting a preliminary decision support system to the medical practitioners.

Acknowledgment

First and foremost, I would like to thank God Almighty for his grace, guidance, and blessings. Thank you, Lord, for the power that you have given me to believe in myself and the passion to pursue my dreams.

During this expedition of my doctorate research, I have been blessed by the support of many special people who have always inspired and motivated me. Words can never be enough for expressing my gratefulness and respect to all those special people in my life who made this research possible.

I am very grateful to my supervisor Dr. Priyanka Sharma, Professor and Head of IT department at Raksha Shakti University, especially for her constant patience, ongoing support and encouragement throughout the past four years. Her enthusiasm, constructive criticism, research ideas and always making time for discussions have made the completion of my research possible and highly enjoyable. I am privileged to have worked with her.

The completion of this work would not have been possible without, the Doctorate Progress Committee (DPC) members: Dr. Sanjaykumar Vij, Dean (CSE, MCA, and MBA) ITM Universe and Dr. Bankim Patel, Director of SRIMCA, Uka Tarsadia University. I am really thankful for their rigorous examinations and precious suggestions during my research.

The Ph.D. Department at the Gujarat Technological University has been an excellent place to conduct research, and all members of staff and colleagues have been encouraging and helpful whenever needed. My gratitude goes out to the assistance and support of Dr. Akshai Aggarwal, Ex-Vice Chancellor of GTU, Dr. Rajul Gajjar, Ex. Dean, Ph.D. Programme, Dr. Navin Sheth, present Vice-Chancellor of GTU, Dr. N. M. Bhatt, Dean, Ph.D. Programme, Mr. J. C. Lilani, I/C Registrar, Ms. Mona Chaurasiya, Research Coordinator, and other staff members of Ph.D. Section, GTU.

Most importantly none of these would have been ever possible without my loving, supportive, encouraging, and patient husband Rushabh. His unceasing faith and support helped me survive all the stress for all these years and let me not give up. He has been non-judgmental of me and instrumental in instilling confidence in me. These past several years

have not been an easy ride, both academically and personally. I truly thank him for sticking by my side, even when I was irritable and depressed. His love and trust in me were the driving forces which gave me the inspiration and stimulus during all stages of my research. I feel that we both learned a lot about life and strengthened our commitment and determination to each other and to live life to the fullest.

I owe a lot to my parents, who raised me with love and encouraged and helped me at every stage of my personal and academic life. I would like to thank my parents for supporting me spiritually and emotionally throughout writing this thesis and my life in general.

I wholeheartedly thank my mother-in-law and father-in-law who supported me immensely. It is their unparalleled love and good wishes that worked along with me on this journey.

My lovely son, I love you with my entire heart and soul! I thank you for the light and joy you have brought to my life. You changed my life for better and welcomed me into motherhood. An incident with you had been the biggest motivation for me to take this research project. You are the main inspiration and motivation for my research dear son. Stay Blessed!

I would take this opportunity to thank the many people who have taught me starting with my school teachers, my undergraduate teachers, and my post graduate teachers. I have to give a special mention for the support given by my colleagues and fellow Ph.D. Scholars. They have all extended their support in a very special way, and I gained a lot from them, through their personal and scholarly interactions, their suggestions at various points of my research.

I would like to address special thanks to the reviewers of my thesis, for accepting to read and review this thesis and giving approval of it. I would like to appreciate all the researchers whose works I have used, initially in understanding my field of research and later for updates. I am very grateful to the authors of various articles on the Internet, for helping me become aware of the research currently ongoing in this field.

I also extend my hearty thanks to all those who have directly or indirectly helped me in the journey of my doctorate research.

Thank you.

DEDICATED TO,

My Mother,

Whose dream was to see me pursue doctorate

My Son, Aarush

The main motivation behind my research

TABLE OF CONTENTS

List of Abbreviation

MODS	Multiple Organ Dysfunction Syndromes
ROI	Region of Interest
RG	Region Growing
ROIMI	Region of Interest in Medical Imaging
USG	Ultra-Sonography
ASM	Active Shape Model
AAM	Active Appearance Model
RGB	Red, Green, Blue Colour Model
GIMP	GNU Image Manipulation Program
SDF	Signed Distance Map
PDE	Partial Differential Equation
BWB	Black White Black
CFL	Courant Friedrichs Lewy
DICOM	Digital Imaging and Communications in Medicine
CDSS	Clinical Decision Support System
DSS	Decision Support System
MRI	Magnetic Resonance Imaging

List of Figures

List of Tables

CHAPTER – 1

Introduction

1.1 Introduction to the X-Ray imaging

Bone fractures are very common in our country today. Fractures are the major type of injury caused by a bad fall, sports or road accidents. Fracture is a medical condition which leads to break in the continuity of the bone. Patients with bone fractures who go into shock state have a mortality of 30-50%. In some cases, when combined with other injuries in the body, for example, an abdominal injury, the chance of mortality rises even higher, approaching 100%. Other conditions which can result in higher mortality rate are severe hemorrhage due to severe traumatic injury in the fracture region, multiple organ dysfunction syndromes (MODS), injury to the nerves, internal organ damage, thus resulting in a higher mortality rate.

According to the market report of India Today [1], the Indian hospitals have the highest record of fractures and this has increased 3-folds over the past few decades. There have been 4.4 lac people suffering from bone injuries in last 3 decades and is expected to increase to more than 6 lack by 2020.

The X-Ray images are the most common imaging accessibility for people suffering injuries during the accidents. X-rays are the oldest and most frequent form of medical imaging. But the minute fracture detection in the X-Ray image is not possible due to the complexity of bone structure and the difference in visual characteristics of fracture by their location. So it

is difficult to accurately detect and locate the fractures and also determine the severity of the injury. The numerous incidences necessitate the health care professionals to analyze a huge number of X-ray images. A significant portion of diagnostic errors arises through cognitive errors resulting from inadequate knowledge, faulty diagnosis, and/or faulty verification. Experts estimate that 75% of diagnostic failures can be attributed to clinician diagnostic thinking failure[2]. In today's revolution oriented medical environment, computer-aided disease detection can play a vital role in a wide range of medical applications and services.

The automatic detection of fractures in X-Ray images can be a significant contribution to assisting the physicians in making faster and more accurate patient diagnostic decisions and treatment planning.

Among fractures, automatic detection is considered more challenging because they are different and variable in presentation and their outcomes are unpredictable. The major challenges in medical imaging are 1) the segmentation process, 2) automatic identification of the region of interest 3) evaluation 4) suggestive course of action. Segmentation allows the partitioning of an image into regions with cohesive properties.

The main aim of this research work is to minimize diagnostic errors, by providing an automatic identification of the region of interest (bone breakage) along with preliminary decision support system.

The research proposes an automatic algorithm (ROIMI) for detecting bone fracture in the X-Ray image. The algorithm will automatically identify the region of interest (bone breakage). It will evaluate the type of breakage from the region of interest identified based on its size and also suggest the immediate course of treatment required. The results of this novel system are promising, demonstrating that the proposed algorithm is capable of automatically detecting hairline, minor and major types of fractures accurately, and shows potential for clinical application.

1.2 Motivation:

One fine night at around 11:00 P.M, one boy of 2 years was playing joyfully with his father. The boy was climbing on the back of his father and jumping on the bed and

laughing loudly. The father was very happy watching his son play. Once again the boy jumped on the bed, but this time he did not laugh. While jumping the boy could not balance and get hurt. There was a severe swelling in his hand which indicated that there must be a bone breakage. The father rushed him to the near most orthopedic hospital. As it was the late night the doctor was not available. The attendant at the hospital took the X-Ray, but could not understand what treatment should be done. So he called up the doctor. It took more than an hour for the doctor to reach the hospital and start the treatment. The boy had suffered a major fracture. As the boy was young only fixation and casting would have cured his fracture but the delay in the treatment resulted in surgery.

Such delay in treatment for adults and elderly people can prove to be fatal. The especially surgical delay is associated with a significant increase in the risk of death. Certain fractures can cause severe hemorrhage or predispose to other life-threatening complications. Femur fractures that disrupt the femoral artery or its branches are potentially fatal. Patients with multiple rib fractures are at substantial risk for pulmonary contusion and related complications.

All these facts have motivated us to develop the proposed fracture identification and detection system that can automatically determine the presence and absence of fractures and if present with the aid of the decision support system can suggest the immediate course of treatment for the fracture.

1.3 Objectives

The main focus of this work is to automatically detect a region of interest (bone fracture) from the bone X-ray images and in particular suggest the course of treatment based on the type of crack identified in the region of interest using a series of sequential steps. The objectives can be stated as follows:

1. To extract the bone part from the X-ray image.
2. To develop an algorithm that automatically identifies the region of interest (the breakage in bone) in the image.
3. To develop an algorithm to analyze and evaluate the type of breakage.
4. To develop decision support system to suggest the course of action based on the type of breakage.

1.4 Organization of Thesis

Thesis organization for rest of the chapters is as follows:

Chapter-2 provides an extensive literature survey on medical imaging modalities, medical image segmentation methods, and challenges associated with the automated segmentation of bone from the X-ray image. It also discusses the need and challenges for computer-aided detection of fracture in bones.

Chapter 3 discusses various image preprocessing methods performed to achieve better and more accurate segmentation. It also explains the current methods being used in the field of image segmentation and the need for diagnostic decision support systems.

Chapter 4 describes the methodology used in the algorithm.

Chapter 5 gives detail steps of the algorithm, flowchart and the simulation screens of the developed application.

Chapter 6 displays the results obtained and discussions related to the results.

Chapter 7 conclude the thesis with some suggestions for future work.

CHAPTER – 2

Literature Survey

2.1 Medical Imaging

Today in the healthcare domain, medical images play a vital role. Medical imaging is of significant use in the process of diagnosis, treatment planning, surgical procedures and follow up studies. Medical imaging can be defined as the process of representing visually the interior parts of body, tissues or organs for clinical analysis, treatment, and disease monitoring.

Various digital medical imaging methods like computed tomography (CT), magnetic resonance imaging (MRI), ultrasound, PET (positron emission tomography), SPECT (single photon emission computed tomography), etc. have all become important to medical practitioner's arsenal of imaging tools toward more reliable detection and diagnosis of disease.

Table 2. 1 Different Types of Medical Images and its Purpose

Sr No	Medical Imaging Type	Purpose
1	Ultra-Sonography (USG)	To record images within the body ultrasound is used
2	X-Ray	Uses X-Ray beam to record images of internal bone structures of the body.
3	Echocardiography	It is used to know the heart state.
4	Computer Axial Tomography Scan	To know the state of the interior organs in slices.
5	Magnetic Resonance Imaging	It is used to get more clear images than CT Scan.
6	Linear Accelerator	It is used for radiotherapy in cancer.

The research focusses on finding the Region of Interest in the bones of X-Ray images.

So the further explanation would be concentrating on X-Ray images.

2.1.1 X-Ray Imaging

X-Ray imaging is the oldest and the most commonly used form of medical imaging. X-Ray imaging uses X-Ray beams that are projected on different parts of the body. The X-Ray beams are absorbed in different amounts depending on the density of the organs while passing through the body. On the opposite side of the body, the X-Rays are detected resulting in an image. The following figure shows a sample Chest X-Ray image.

Figure 2. 1 Chest X-Ray

Table 2. 2 Parts of Chest X-Ray

Fat	**Appears Dark Grey**
Air and gas	**Appears Black**
Soft tissue and water	**Appears Light Grey**
Contrast Material and Metal	**Appears Bright White**
Bone	**Appears Light White**

X-Ray images are typically used to treat:

1. Broken Bones
2. Cavities
3. Breast Cancer
4. Swallowed objects
5. Lung diseases
6. Identification of stones in the urinary system
7. Problems in abdominal organs

The research focusses on different types of bone fractures. Significantly for our work,

X-Rays are the images used for analysis.

2.1.2 Bone Fracture types

Bones in the human body are naturally rigid and normally it cannot bend. An outside force can cause a bend in the bones, and when the force is too high, the bone will break or will get fractured/cracked. Bone fractures are of several types and the classification depends on the injuries caused by the breakage of the bone.

Regardless of the cause, generally bone fracture can be of following two types:

1) **Simple fractures**

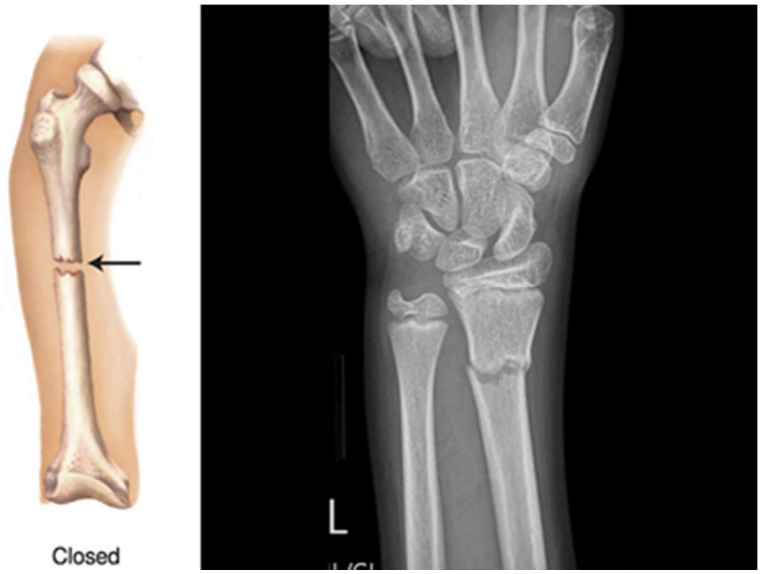

Figure 2. 2 Simple Fracture

Simple fractures are the closed fractures, as the broken bones stick inside the skin. It may be just a crack rather than the break.

2) Compound fractures

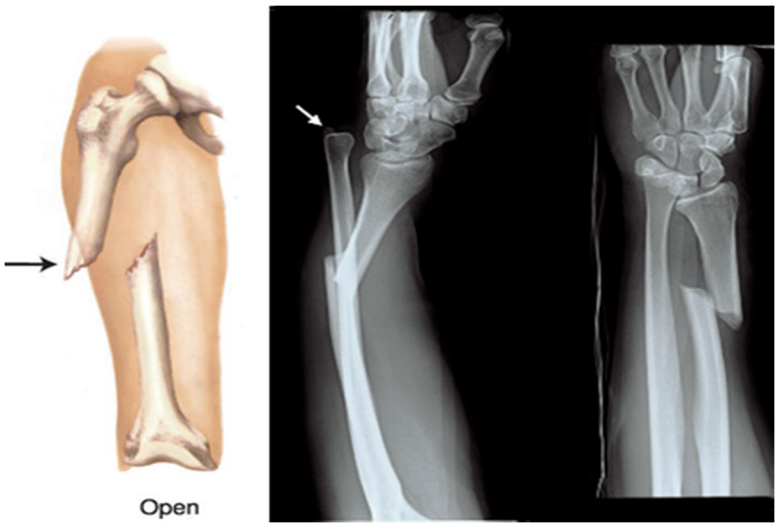

Figure 2. 3 Compound Fracture

Compound fractures are highly critical as the broken bones penetrate out through the skin. They are also known as Open fractures. Compound fractures are highly prone to infection as the skin is cut. There is a possibility of infection in the place of wound and bone.

Other types of fractures also can be classified as follows.

3) Transverse fractures

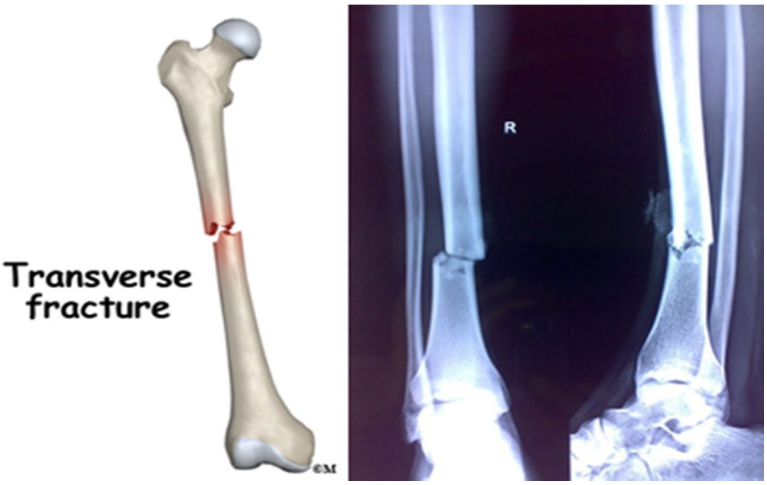

Figure 2. 4 Transverse Fracture

Bone Crack/break from the right angle to the bone's long axis.

4) Spiral fractures

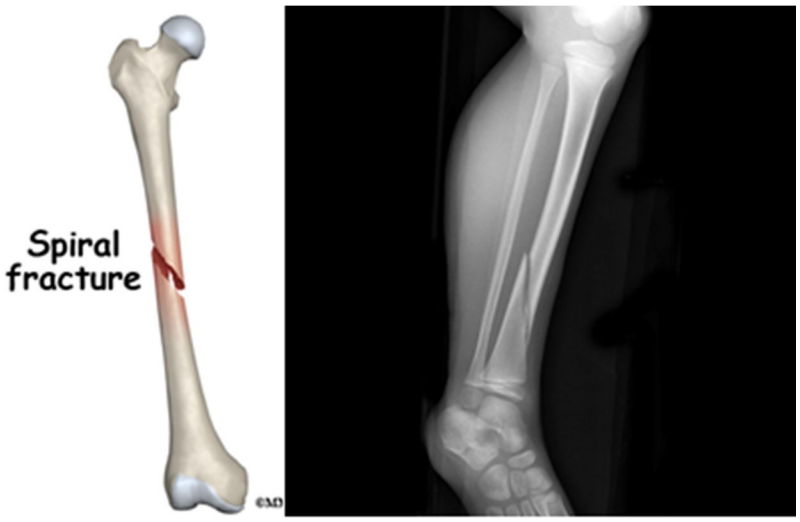

Figure 2. 5 Spiral Fracture

When the bone is twisted by extreme force then this type of bone fractures occurred. In Spiral fractures, the bone is broke in the twisted pattern.

5) Comminuted fractures

Figure 2. 6 Comminuted Fracture

Comminuted fractures are severe fractures in which bone is broken apart into several small pieces.

6) Impacted fractures

Figure 2. 7 Impacted Fracture

In impacted fractures, broken bone fragments are collapsed with each other. The external force is too extreme that bone fragments submerge into each other.

7) Greenstick fractures

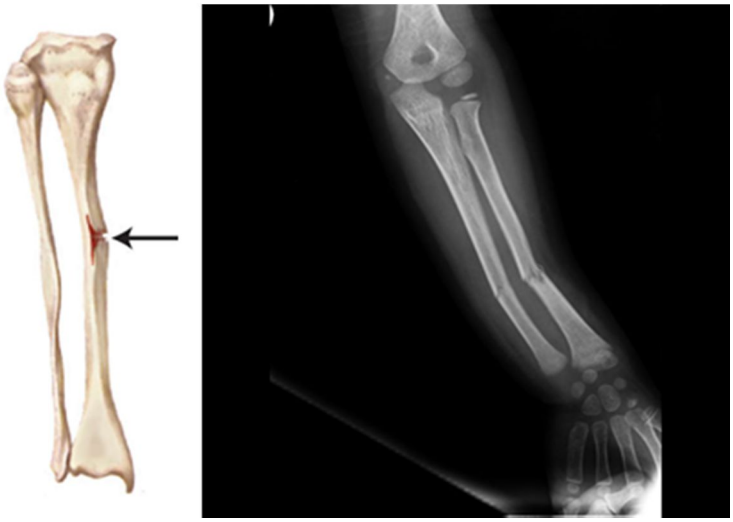

Figure 2. 8 Green Stick Fracture

Generally, this type of fracture is seen in the developing bones (i.e. children bones). Only one side of the bone got fractured and the other side may be bend.

8) Oblique fractures

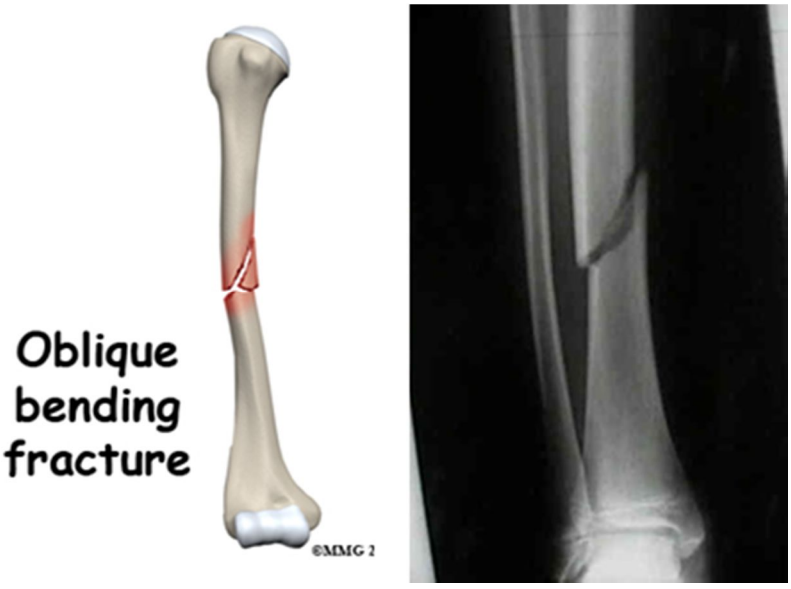

Figure 2. 9 Oblique Fracture

This type of fracture is Diagonal to a bone's long axis. The external or accidental force is applied to the bone other than the right angle and it will cause the oblique fracture.

2.2 Medical Image Segmentation

Medical Image Segmentation has numerous applications. It can be either a part of any decision support system or some other quantitative analysis to be done. It has thusly pulled in a lot of consideration resulting in a vast literature of published reviews and computational techniques.

2.2.1 General Approaches to Segmentation

There are different approaches to Segmentation but it can be categorized mainly into three different types. Automatic segmentation, semi-automatic segmentation, manual segmentation.

In manual segmentation generally it is done by human and most of the time it is accurate but it will consume a lot of time.

In semi-automatic segmentation user inputs will be required in a certain degree and then based on user inputs segmentation will be performed. An example can be specifying parameters to the clustering algorithm.

Automatic segmentation is the toughest of all the three type of segmentation because it does not involve any user input. But it has the biggest advantage that it will be less time to consume as it can process a large number of images without user inputs. The only major thing would be to provide automatic segmentation algorithm which is quite efficient.[5]

Withey divides the medical images segmentation into three generations where each adds an additional level of algorithmic complexity.[6]

One of the generation techniques which are of the first generation works on a low level like finding pixel intensity values or on bimodal thresholding using Otsu's method[7], edge tracing, and region growing based on homogeneity of adjacent pixels. Here the approaches do not use any prior information and so they are of limited use.

Some methods which fall under the second generation uses statistical analysis. Here pixels in the image can belong to the known class of a predefined set. Here methods like active contour or snakes can be used which can either expand or contract towards the specific features, in the image[8].

The latest generation calls for the third generation works with the prior information supplied to it and are faster. Two of the best known are Active Shape Model (ASM) and Active Appearance Model (AAM)[9]. Methods mentioned here are supervised learning methods as it requires a set of labeled training images.

2.2.2 Segmentation of bone from X-ray Images and its literature survey

As seen in the past literature X-Ray has got relatively less attention. This can be due to the fact that X-Ray images are very difficult to analyze. Also, there are huge variations in X-Ray images that are taken due to the fluctuations in the photon density of the X-Ray beam. Also, noise is generated which results in intensity variation and contrast which does not

keep the quality of the image same always for the same organs X-Ray also[10].

There is difficulty in identifying the organ, skin and bone part in the X-Ray image because of absorption rate by different tissues and also it leads to blurred edges in the image. Also for two different persons or patients, the same X-Ray taken of the same organ of the body has different intensity characteristics which make it challenging for the researcher to do the research on the same part of the bone.

A patient with osteoporosis will have diminished bone thickness, and bone matter in the influenced region will thusly seem darker than typical in X-Ray pictures. Thus, however, the general structure continues as before, the exact state of bones may differ starting with one patient than the next. This is muddled further by pose changeability. In instances of traumatic injury, it may not be advisable to move the patient into the perfect position when taking X-Ray pictures, especially in the event that he/she is in an unsteady condition or has managed the various injury.

The area and introduction of particular structures may hence shift starting with one X-Ray picture then onto the next, notwithstanding when gathered from a similar patient. An issue of specific pertinence in pelvic radiographs is cover between bones, which causes obscured limits and trouble portraying bone matter from delicate tissue and organs. Pelvic X-Rays are inclined to another particular confusion. The nearness of gas inside the colon, which makes dim shadows show up over the iliac fossa.

One of the studies for radiograph segmentation by Manos[11] has gone with region-growing and merging method according to the size, similarity and then was assigning labels corresponding to different regions according to intensity characteristics. Limitation of the approach by him was neither he has considered spatial information. Also, regions were not clearly demarcated according to those studies for different images of X-Ray.
Some early studies also focused on identifying lung regions in chest X-Rays and they applied Markov Random field models[12], rule-based heuristics[13], and classifiers based on local features [14] with a different rate of success.

One study has applied ASM for automatic segmentation of the patella in knee joint[15] with the help of a genetic algorithm. But as patella is very simple structure to identify with

clearly defined edges it might be difficult to obtain good results in the case when there are overlapping structures. Tragically, this caveat applies to a large number of the reviews that utilize ASM or AAM to recognize objects of interest for pelvic X-Ray images. But in recent times deformable models have gained importance in automatic as well as semi-automatic segmentation methods. Example applications include detecting vertebrae fracture[16]and isolating lung fields in chest radiographs[17], [18]. For instance, the computerized division technique proposed by Boukala[19] regards the pelvis as a single structure and can't recognize singular bones; moreover, the shape setting descriptors it uses to introduce the model are helpless against spurious edges in the information images.
Region Growing (RG) technique is a region-based segmentation method which is applied locally to an image[20]. RG analyzes pixels in a neighbor of physically or consequently set seed points and combines them if a homogeneity condition in intensity similarity is met. RG strategies are utilized primarily to segment the knee bone[21] because of its bigger measurement in the joint and they are more powerful than thresholding techniques[22], [23]

Deformable models are semi-automatic techniques that are broadly utilized as a part of clinical applications. The division is obtained by distorting a flexible contour which develops toward the object by image forces. Example of it can be balloons, snakes and active contour[8], [24]

Some advanced segmentation method based on atlases is a combination of less advanced methods with the latest one[25]. Atlas methods which are based on intensity, shape, and texture are hybrid segmentation methods[26][27]. Here source image is converted to the target image using non-linear geometrical transformations giving reliable results.

Ding [28] use of an atlas-based approach in automatically segmenting the femurs from AP pelvic X-Ray. Images with multiple overlapping bones always present a greater technical challenge to segment the bone part from the image. Thus by studying the above literature, it is difficult for the machine to automatically segment the part of the bone from the X-Ray image.

2.3 Automatic Identification of Region of Interest (bone breakage)

The most difficult part of medical image analysis is the automated localization and delineation of structures of interest. Automated data evaluation is one way of enhancing the clinical utility of measurements. A crucial role for automated information extraction in medical imaging usually involves the segmentation of regions of the image in order to quantify volumes and areas of interest of biological tissues for further diagnosis and localization of pathologies.

A bone x-ray makes images of any bone in the body, including the hand, wrist, arm, elbow, shoulder, foot, ankle, leg (shin), knee, thigh, hip, pelvis or spine. Detection and correct treatment of fractures are considered important, as a wrong diagnosis often leads to ineffective patient management, increased dissatisfaction, and expensive treatment. During literature survey, we did not get any such research paper addressing automated identification of the bone fractures from the X-ray images. However, only a few inventions have claimed automated segmentation of the bone part from the X-ray image. Patent No: US9275469 US claims compositions and methods that allow for the analysis of bone mineral density and/or bone structure from x-ray images, wherein the bone structure includes trabecular bone structure. Patent No: US 8715187 B2 claims at automatically identifying and segmenting different tissue types in ultrasound images. Patent No: US 8135200 B2 relates to an imaging system using auto-shutter, a method for finding a region of interest in a digital image.

2.4 Decision support system

The importance of automated fracture detection comes from the fact that in clinical practice when an orthopedic doctor is not available, it becomes difficult in providing timely treatment. This can lead to fatal consequences.

Computer detection of fractures can assist in identifying the type of fracture and the decision support system can give the primary course of treatment and thus improve the timeliness and fasten the healthcare for the patient.

CHAPTER - 3

Medical Image Pre-processing, Segmentation, and Decision Support System

3.1 Medical Image Pre-processing Methods

Present day's Medical science largely depends on the medical imaging technologies like X-Rays, MRI, CT, Ultrasound etc. for diagnosis and treatment planning. Medical practitioner's use this images for the study of different organs of human body. But, generally medical images are not only complex but they also contain noise. Due to extensive use of medical images for diagnosis, treatment planning and further tracking of medical disorders, the importance of medical image processing has also increased. Medical image processing follows various steps like de-noising, image enhancement, delineating, registration, segmentation, etc. for precise study of an image[20, p. 6]. Segmentation is the process of partitioning an image into more meaningful regions for ease of analysis[31].

The first step towards image processing is filtering noisy images. Noise is introduced into medical images due to errors during the image transmission and capturing process. The quality of medical images may vary due to non-uniform intensity levels, noise, or overlapping of different organ parts[31]. Noise may reduce the visibility of some structures and objects, especially those that have relatively low contrast. This indicates the

importance of image de-noising and image enhancement before the segmentation. De-noising and enhancement are pre-processing steps, as they occur before segmentation. This image pre-processing steps are fundamental to ensure high accuracy of subsequent steps.

Image pre-processing is specifically more significant for bone segmentation task so that the further steps of the algorithm of feature extraction work correctly. Thus, proper detection and segmentation of the bone lead to exact extraction of features and classification of bone fractures.

Need for pre-processing of Bone X-Ray images[32]:

- It makes images more suitable for further processing steps.
- It enhances the image quality.
- It removes noise from the image.

Pre-processing stage performs several steps to improve the quality of the image:

3.1.1 Image de-noising:

Image de-noising helps in noise reduction, interpolation, and re-sampling. It is challenging to remove the noise from the image while preserving the details of the image. Through previous work, it has been observed that the choice of filters for de-noising the medical images depends on the type of noise and type of filtering technique used.[33] Best suited filtering techniques which smoothen the image under analysis without affecting the image quality are employed.

The function of filters is to suppress either the high frequencies in the image, that is smoothing the image or the low frequencies that is enhancing or detecting edges in the image. [13]. Various filtering techniques which eliminate noise without any loss of important information are:

Mean filter:

If there is much intensity variation between one pixel and another then we can go for applying Mean filtering which takes the average of nearby pixels and replaces the value of this pixel. It can be used for smoothing edges. This has the effect of eliminating pixel values which are unrepresentative of their surroundings[34].

Wiener filters:

When the noise is high in image Weiner filter is used. This method uses the information about the band of the noise and the original signal. Wiener method implements spatial smoothing and corresponds to appropriate choice of the window size[35]. The Wiener filtering method requires the information about the bands of the noise and the original signal. [36].

Median filter:

As the name suggests this type of filter takes the median of the neighboring pixel and replace the value of the original pixel. This filter can replace the original gray level of the pixel by taking median. This filter is popular for reducing noise without blurring edges of the image[34]. The median filter is very useful to reduce salt and pepper noise and speckle noise. It is particularly useful in the case where edge preservation is desirable.

Gaussian filter:

The Gaussian filter is normally used as an image smoother. Mathematically, a Gaussian filter modifies the input signal by convolving with a Gaussian function. The output of the Gaussian filter at the moment is the mean of the input values.

Kalman Filter:

A Kalman filter is an optimal estimator. This means that it infers parameters of interest from indirect, inaccurate and uncertain observations. It is recursive so that new measurements can be processed as they arrive. In case if noise is Gaussian, the Kalman filter will minimize the mean square error of the estimated parameters. [37]

3.1.2 Converting to grayscale:

To enter the next stage of image processing the X-Ray image must be converted to grayscale. The X-Ray image is an RGB that essentially does not contain many colors, so converting to grayscale will not significantly reduce the important information of the image.

3.1.3 Image Enhancement:

Image enhancement is the simplest and most appealing step of digital image processing. This process improves the quality of the image to obtain good results. Image enhancement methods help to bring out the obscured details of the image simply by highlighting certain features of interest in an image. This is done by changing brightness or contrast etc. values of the image pixels.

3.1.4 Image Restoration:

The main function of image restoration process is to improve the appearance of an image. Image enhancement step is subjective, but image restoration step is objective, as the image restoration methods are based on mathematical or probabilistic models which are related to image degradation.

3.1.5 Edge detection:

The points which exhibit a sharp change in the brightness and are clustered into sets of curved line segments can be termed as edges in an image. Typically a sudden change in the discontinuities in an image is known as edges. Edge detection is a process of finding this intensity changes in an image. Edge detection is a fundamental tool in image processing, particularly when the further steps involve feature detection and feature extraction[38]. Edges are the points which define the boundaries between different regions in an image. Hence edge detection can be fundamental for segmentation and object recognition. Edge detection in an image can significantly reduce the amount of data as it filters out non-important regions while preserving the information and structural properties of important regions in an image.

An edge detector is basically a high pass filter that can be applied to extract the edge points in an image[39]. There are many edge detection methods in use. These methods are categorized based on the approaches they use as[40], [41]:

1. Gradient-Based Approaches
    a. Sobel
    b. Prewitt
    c. Roberts
2. Laplacian-based Approaches
    a. Marr-Hildreth Algorithm
3. Canny Algorithm

Gradient-based approaches like Sobel, Prewitt, and Roberts detect edges by first computing a measure of edge strength, which are usually a first-order derivative expression such as the gradient magnitude, and then searching for local directional maxima of the gradient magnitude using a computed estimate of the local orientation of the edge. Whereas the Laplacian-based approaches and Canny Algorithm search for zero crossings in a second-order derivative expression computed from the image in order to find edges. They are usually the zero-crossings of the Laplacian or the zero-crossings of a non-linear differential expression.

The intensity differences and the edge detection operators used have a significant effect on the edge detection output.

Sobel Edge Detection:

The Sobel edge detection method is introduced by Sobel in 1970 [41]. The Sobel method of edge detection for image segmentation finds edges using the Sobel approximation to the derivative. Sobel operator is used to calculating the gradient of image intensity. It finds the direction of possible increase from light phase to dark phase and the rate of change in the direction.[39] It precedes the edges at those points where the gradient is highest.

-1	0	+1
-2	0	+2
-1	0	+1

Gx

-1	-2	-1
0	0	0
+1	2	+1

Gy

Figure 3. 1 Vertical and Horizontal Mask using Sobel

The operator consists of a pair of 3×3 convolution kernels as shown in Figure 3.1. One kernel is simply the other rotated by 90°. The kernels can be applied separately to the input image, to produce separate measurements of the gradient component in each orientation (*Gx* and *Gy*).

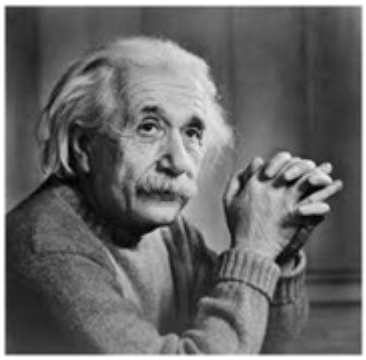

Figure 3. 2 Original Image

Figure 3. 3 Edge Detection by using Vertical Mask of Sobel

Figure 3. 4 Edge Detection by using Horizontal Mask of Sobel

Robert's edge detection:

The Roberts edge detection is introduced by Lawrence Roberts (1965). [41] It performs a simple, quick to compute, 2-D spatial gradient measurement on an image.[42] Pixel values at each point in the output represent the estimated absolute magnitude of the spatial gradient of the input image at that point.

The operator consists of a pair of 2×2 convolution kernels as shown in Figure 3.5. One kernel is simply the other rotated by 90°. This is very similar to the Sobel operator.

+1	0
0	-1

Gx

0	+1
-1	0

Gy

Figure 3. 5 Vertical and Horizontal Mask used in Robert's

Prewitt Edge Detection:

The Prewitt edge detection is proposed by Prewitt in 1970 [41]. Edges are calculated by using the difference between corresponding pixel intensities of an image. All the masks that are used for edge detection are also known as derivative masks.

-1	0	+1
-1	0	+1
-1	0	+1

Gx

-1	-1	-1
0	0	0
+1	+1	+1

Gy

Figure 3. 6 Vertical and Horizontal Mask in Prewitt

It is a first order derivate and calculates the difference of pixel intensities in an edge region. This gradient-based edge detector is estimated in the 3x3 neighborhood for eight directions. All the eight convolution masks are calculated. One complication mask is then selected, namely with the purpose of the largest module.[39].

Figure 3. 7 Edge Detection by using Vertical Mask of Prewitt

Figure 3. 8 Edge Detection by using Horizontal Mask of Prewitt

The comparison of the Sobel operator and Prewitt operator shows that Sobel operator finds more edges or make edges appear more clear and visible than Prewitt operator. This is because Sobel operator has allocated more weight to the pixel intensities around the edges.

Laplacian-based Approach

Laplacian operator also calculates the gradient but it searches the zero crossings in the second order derivative to identify the edges in an image.

Marr-Hildreth Algorithm:

The Marr-Hildreth (1980) technique is a method of detecting edges in digital images. It first smoothens the image by using a Gaussian smoothing operator to improve the response

to noise. Then it applies a two-dimensional Laplacian to the smoothed image. It then loops through the result and looks for changes in sign. If there is a change in sign and the slope across the sign change is greater than some threshold, it will mark it as an edge.

Canny Algorithm

The Canny algorithm was developed by John F. Canny in 1986. It is mainly used to find many edges in the image.

The steps of the multistage Canny edge detection algorithm are 1. The Gaussian filter is applied to smooth the image and to remove the noise. 2. The intensity gradients of the image are calculated. 3. Non-maximum suppression is applied to get rid of false response for edge detection. 4. The double threshold is applied to determine possible edges. 5. Edge by hysteresis is used to suppress all other edges which are weak and not connected to strong edges. This will lead to finalization and detection of potential edges.

An upper threshold and a lower threshold are the two key parameters of the algorithm. The upper threshold identifies the absolute edges whereas the lower threshold finds the faint pixels that are actually a part of an edge[43].

In practical use, the Canny edge detection is one of the standard edge detection methods as it outperforms many of the newer algorithms that have been developed after Canny[42]. Canny is one of the important methods as it finds the edges by separating noise before from the image before find edges of the image[44].

3.2 Medical Image Segmentation

Image segmentation is the process of partitioning the image into a group of pixels having same characteristics. The main goal of image segmentation would be to partition the image in such a way that it would make it more meaningful and easier to analyze the image.

Image segmentation is used to partition a digital image into multiple segments. This segments may be a set of pixels, pixels in a region are similar according to some homogeneity criteria such as color, intensity or texture, so as to locate and identify objects and boundaries in an image[40], [41].

The major practical applications of image segmentation are:

- Face Recognition,
- Medical applications like locating tumors, fractures and other pathologies, Measure tissue volumes, diagnosis, treatment planning, computer-assisted surgery, the study of anatomical structure etc.
- Filtering of noisy images,
- Fingerprint Recognition,
- Locate objects in satellite images like roads, forests, etc.,

The goal of image segmentation is to simplify or change the representation of an image into something that is more meaningful.

3.2.1 Reasons for using Segmentation

For many applications, the user may want to group pixels together based on certain characteristics. The characteristics can be intensity, color, shape etc. according to the applications. In medical images to group certain region having same characteristics segmentation is employed. As there is no established ground truth of the image we have to perform segmentation differently for different medical images. If an image is presented to ten different users and if they are told to perform manual segmentation then they might end up with ten different solutions. So again it is a problem when the user goes for automatic segmentation.

For human beings, the image is perceived as a whole and the segmentation of a part of the image is an easy task. But for machines, the image is a matrix filled with numbers. The machine does not have a clue what the number represents and so it is a difficult task for the machine to segment the image. Our approach is to segment the bone part form the X-Ray image. To segment, the bone from the image is a very tough part as it consists of soft tissues, noise, and different image contrast and also data ambiguity. We cannot have same intensity values for each and every X-Ray images. Segmenting the bone from the X-Ray is always a part of research and it is difficult for anyone algorithm to work for segmenting a bone part from the image.

3.2.2 Medical Image Segmentation Methods

Image segmentation can be classified according to various types based on intensity discontinuities, intensity similarity and morphological features of the image. The choice of a segmentation technique and the level of segmentation depends on the particular type of image and characteristics of the problem being considered. The Segmentation approaches proposed in the literature are shown below in Table 3.1.

Table 3. 1 Medical Image Segmentation Methods

Segmentation Methods	Thresholding	Otsu EGT Background Subtraction Thresholding of Morphological Gradient Local Adaptive Thresholding SCT	
	Region-Based	Region Growing	Seeded Region Growing
	Energy Based	Active Contours	Level Sets 3D Snakes Active Mesh
		Graph-Based	Random Walk Minimum Cut
	Region and Contour Based	Watershed	H-maxima Transform Marker-based Watershed
	Morphological	Subsequent Dilation Ultimate Erosion	
	Partial Derivative Equations (PDE)	Levenberg and Marquardt Minimization Multistep with Watershed	

3.2.2.1 Thresholding

Thresholding is one of the simplest and most commonly used techniques used for image segmentation. Thresholding divides the image into separate regions based on their intensity values. The image is segmented into two regions depending on their intensities as one

region that becomes the background and the other region that becomes the object. To determine what cluster a pixel belongs to, following formula is used:

$x \subset C1$ if intensity(x)>threshold

$x \subset C2$ if intensity(x)≤ threshold

Where x is the pixel and intensity(x) is the grayscale value for that pixel.

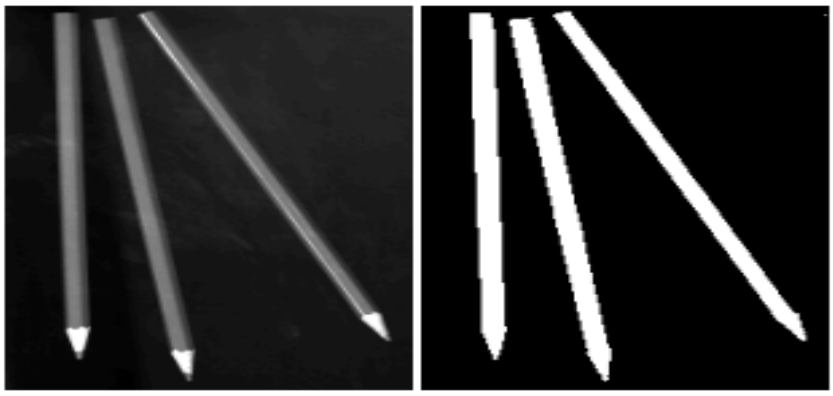

Figure 3. 9 Example of Segmentation by Thresholding

The difficult task with thresholding methods is to determine the threshold values which can best differentiate the regions of interest. For example, if the selected threshold is too low, pixels that are supposed to be background gets labeled as being part of the objects, and if the selected threshold that is too high, pixels that should be the object gets marked as background. To overcome this difficulty there are ways to automatically determine an appropriate threshold, like Otsu's method[9]. Thresholding can be extended to divide the image into more than two regions by using multi-threshold values. It can also be extended to color images by thresholding each color value in the image.

Adaptive thresholding methods are used to segment images that are noisy or have intensity in-homogeneities like MRI images. They are also known as local or dynamic thresholding methods[45], as they compute a distinct threshold for each pixel or voxel based on the local image properties.

3.2.2.2 Edge based segmentation

Edge-based segmentation is the most common method based on detection of edges i.e. boundaries which separate distinct regions. Edge detection method is based on marking of discontinuities in gray level, color etc., and often these edges represent boundaries between objects.

There are various edge detecting operators available which are based on gradient (derivative) function. They are Prewitt, Sobel, Roberts (1^{st} derivative type) and Laplacian (2^{nd} derivative type), Canny, Marr-Hildreth edge detector.

3.2.2.3 Region-Based Segmentation Methods

Region-based methods are based on the principle of homogeneity: Objects are found by locating their boundaries in the edge-based method, but region based methods follow a dual approach of finding object region instead of its edges. Compared to edge detection method, segmentation algorithms based on the region are relatively simple and more immune to noise.

Region-based methods partition an image into regions that are similar according to a set of predefined criteria. Segmentation algorithms based on region mainly include following methods:

Segmentation algorithms based on region mainly include following methods:

Region growing

This method groups pixel in the whole image into sub-regions or larger regions based seeding points that are required to initialize the process. Hence, the segmentation results are dependent on the choice of seeds.

Steps of region growing method are:

1. Selection of a group of seed pixels in the image.
2. Selection of merging criteria such as grey level intensity or color and set up a stopping rule.
3. Regions are grown iteratively by merging the neighboring pixels based upon the merging criterion.
4. This process is continued until all pixels are assigned to their respective regions as per merging criterion.

Split and merge method:

In Region Splitting and Merging instead of choosing seed points, the whole image is divided into a set of arbitrary unconnected regions and then merge the regions, such that they satisfy the conditions of reasonable image segmentation. Region splitting and merging are usually implemented with a theory based on quadtree data.

3.2.2.4 Active Contours

An active contour or snake are digitally generated curves to move within the image to find the boundaries of the object until it best satisfies predefined conditions. They are energy minimizing curves, creating a closed contour around the image object boundaries by means of deformation under the influence of internal forces and external forces. The seed points, the internal energy, and the external energy are taken as the input for the contour extraction process. The seed point is grown in order to match the internal energy with the external energy. These forces control the shape and location of the curve within the image. The internal forces are responsible for smoothness while the external forces guide the contours towards the contour of ROI. It is a recursive process and the iterations are performed to identify the exact region from the image. The snake algorithm is sensitive to noise.

Level Set Method:

An alternative method for defining active contours was introduced by Osher and Sethian[46]. Level Set methods represent the curves as the zero level set. It employs an implicit representation of the contours[47].This technique provides more accurate numerical implementations and also handle topological change very easily.

3.3 Decision support system

Decision Support Systems (DSS) are interactive software-based systems designed to help decision makers by compiling useful information from a various form of data, documents, and personal knowledge, or rules to identify and solve problems and make decisions[48]. **The computerized decision support** systems make decisions based on the clinical practice guidelines. This technique can save the cost of developing the same medical practice guidelines for multiple decision support systems.[49]

3.3.1 Healthcare Decision Support System

Healthcare Decision Support is the much popular system in the field of healthcare today. They are particularly significant in circumstances in which the measure of accessible data is restrictive for the instinct of an unaided human leader and in which exactness and optimality are of significance. Healthcare Decision support systems can aid human cognitive deficiencies by integrating various sources of health information, providing intelligent access to relevant medical knowledge, and aiding the process of structuring health decisions. They can likewise bolster decision among all around characterized options and expand on formal methodologies, for example, the strategies for operations research, measurements, and choice hypothesis. They can also employ artificial intelligence methods to address heuristically problems that are intractable by formal techniques. A healthcare decision support system provides an important, relevant checkpoint based upon the previous diagnostic information.

There are four components of a Healthcare decision support system[50]:

1. The learning base which comprises of assembled data that can be as administer base or case base.

2. The second part is the model base that contains the guidelines for consolidating the standards or relationship in the knowledge base with genuine patient information.

3. The third component is a User interface, from where patient data can be entered into the system and the output can be given to the user for taking a decision.

4. Forth is the database system. Data can be entered by the clinician person and can be verified at last for its correctness.

3.3.2 Clinical Decision Support System:

It is a health information system that is designed to provide physicians with clinical decision support designed to assist clinicians with patient-related decision makings, such as diagnosis and treatment.

CDSS has shown to improve both patient satisfaction and cost of care. There are a wide variety of uses for CDSS in clinical practice. Some of the main uses include assisting with patient-related decision making, determining optimal treatment strategies for patients etc.

3.3.3 Diagnostic Decision Support System:

Diagnostic Decision Support Systems are designed to “diagnose” diseases and conditions based on the parameters given as the input.

How doctors think, reason and make clinical decisions is arguably their most critical skill. In all of the varied clinical domains[51] where medicine is practiced, from the anatomic pathology laboratory to the intensive care unit, decision making is a critical activity. Diagnostic errors are frequent and underappreciated.

A significant portion of diagnostic errors rises from cognitive errors resulting due to inadequate knowledge, imperfect data, and/or poor verification. Experts estimate that 75% of diagnostic failures[2] can be attributed to clinician diagnostic thinking failure. The identification and implementation of strategies for decreasing or preventing such diagnostic errors have become a growing area of interest and research.

CHAPTER – 4

Methodology

4.1 Introduction

This chapter describes various steps that are used in the algorithm to automatically detect the bone and the region of interest. Each and every step of the algorithm will be described with reasons why these steps were necessary for this chapter. The algorithm will be presented in chapter 5.

X-Ray Images acquired are of different types and also they are subject to noise, contrast and intensity variations. So some pre-processing steps will be required to follow whenever an image is presented for bone segmentation.

4.2 Conversion from RGB to Grayscale

The image can be either of Grayscale or of RGB color nature. If it is of RGB nature then it has three matrices one for each Red, other for Green and Blue. Processing on this three different matrices is difficult and also time-consuming. So the first step will be to convert the image into Grayscale such that it will have an only single matrix representing the intensity value. Grayscale matrix intensity range from 0 to 255. Formulas and methods[52] for converting RGB to grayscale is shown in the following table 4.1

Table 4. 1 Methods and Formulas for Converting RGB to Grayscale

Method	**Formula**	**Description**
Lightness	$\frac{Maximum(R,G,B) + Minimim\ (R,G,B)}{2}$	It averages the most prominent colors and the least prominent colors
Luminosity	$0.21\ R + 0.72\ G + 0.07\ B$	It averages the value of R, G, B but it does the weighted average. As human eyes are more sensitive to green color, so green color is weighted more heavily in formula
Average	$\frac{(R+G+B)}{3}$	It simply averages the value of R, G, and B

To explain the above formulas from GIMP (GNU Image Manipulation Program) Documentation [53] images of sunflower are taken.

Figure 4. 1 Original Image

Figure 4. 2 Lightness Method

Figure 4. 3 Average Method

Figure 4. 4 Luminosity Method

From above we can conclude that lightness methods produce more contrast while luminosity method works best in overall terms. Sometimes all the three methods produce the similar result.

To understand in a better way the Figure 4.5 presented below show an Excel Spreadsheet representing value color values and how to convert R, G, B to grayscale. Value or R, G, B are in the leftmost column. The columns are labeled “Li”, “Lu” and “Avg” for the grayscale value of the color using lightness, luminosity, and average method.

Color	Li	Lu	Avg	R	G	B	Li	Lu	Avg
				255	0	0	128	54	85
				255	153	0	128	162	136
				255	255	0	128	235	170
				0	255	0	128	181	85
				0	0	255	128	18	85
				255	0	255	128	71	170
				0	255	255	128	199	170
				128	128	128	128	127	128
				0	0	0	0	0	0

Figure 4. 5 Excel Spreadsheet example showing Conversion from RGB to Grayscale

In the above Figure 4.5, the grayscale color was created in Excel to set the background color to (X, X, X) where X is the grayscale value. For example in the above figure, “Avg” value is 85 the X is 85 and so the color shown is (85,85,85).

So we can say that when X-Ray image is taken as input in our algorithm it will be converted to Grayscale first. It is shown in the following Figure 4.6. For better understanding, only 5x5 pixels intensity values are shown from the entire image. imGRAY shows the final gray values obtained after conversion in the following Figure. 4.6.

```
>> im(1:5,1:5,:)

ans(:,:,1) =

  125  125  126  127  127
  125  125  126  127  127
  125  125  126  127  127
  125  125  126  127  127
  125  125  126  127  127


ans(:,:,2) =

  136  136  137  138  138
  136  136  137  138  138
  136  136  137  138  138
  136  136  137  138  138
  136  136  137  138  138


ans(:,:,3) =

  122  122  123  124  124
  122  122  123  124  124
  122  122  123  124  124
  122  122  123  124  124
  122  122  123  124  124
```

```
>> imGRAY(1:5,1:5)

ans =

  131  131  132  133  133
  131  131  132  133  133
  131  131  132  133  133
  131  131  132  133  133
  131  131  132  133  133
```

Figure 4. 6 Matlab Image showing sample RGB to Grayscale conversion

4.3 Otsu's Thresholding Method

To separate the bone part from the X-Ray image we have to perform thresholding [54]. But before that, we have to separate the background and the foreground. The easiest but trickiest thing is to select the threshold to separate the foreground and the background from the image. It is different in all the images so we cannot pick any one value. So as seen in literature survey Otsu [9] proposed a method whereby we can threshold the image for separating different objects. So now Otsu thresholding method is explained in detail in this section.

Otsu, basically looks at the histogram of the image. Otsu does not look at edges but it sees the pixel values for segmenting so for this reason uniform pixel values are required. If we look at this image (Figure 4.7) of a fingerprint. By plotting the histogram as in Figure 4.8 we can see that histogram is bimodal.

Figure 4. 7 Finger Print Image

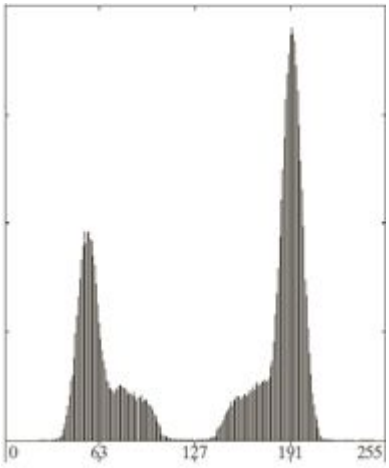

Figure 4. 8 Histogram of Finger Print

A lot of pixels values on the left-hand side of the histogram are of fingerprint and other which are there on the right-hand side of the image are the background. It is very clear from the histogram that there are, two modes in the histogram. So this is a multi-modal histogram. And the basic idea is that if we threshold at the middle point, we can obtain a very simple segmentation, which has separated the fingerprint marks from the background by a simple threshold because we have this bimodal distribution. Otsu, it's going to help us to find basically the threshold in an automatic fashion. The obtained resultant image is shown in Figure 4.9.

Figure 4. 9 Resultant Image using Otsu Thresholding method

Now, of course, not all the time images are as nicely distributed as the above one.

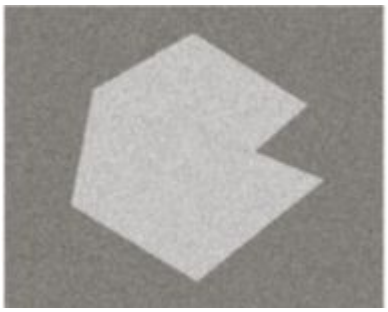

Figure 4. 10 Noisy Image

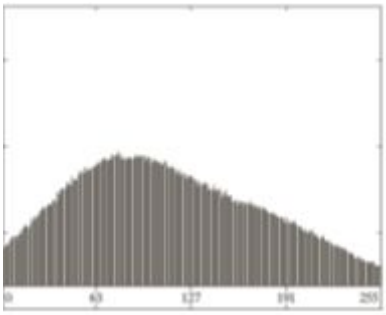

Figure 4. 11 Noisy Image Histogram

If we have an image as in Figure 4.10 with noise and plotting its histogram as in Figure 4.11 we cannot clearly demarcate the separating boundary. Now the histogram is much more distributed. Otsu's method is not going to find a nice threshold. The solution to the above problem lies by denoising the image. We again get back the bimodal histogram and then we can apply Otsu method to it.

The method is trying to find a threshold such that the in-class variability is very small, so method finds a threshold here such that the variance on each one of the classes is as small as possible so the class is as compact as possible. And the methods start from the histogram, and it does not take care of the spacial relationship. What Otsu method does is minimize the weighted within class variance as shown in Equation 4.1 to Equation 4.7.

$$\sigma^2{}_w(t) = q_1(t)\sigma^2{}_1(t) + q_2(t)\sigma^2{}_2(t) \tag{4.1}$$

$$q_1(t) = \sum_{i=1}^{t} P(i) \tag{4.2}$$

$$q_2(t) = \sum_{i=t+1}^{I} P(i) \tag{4.3}$$

$$\mu_1(t) = \sum_{i=1}^{t} \frac{iP(i)}{q_1(t)} \tag{4.4}$$

$$\mu_2(t) = \sum_{i=t+1}^{I} \frac{iP(i)}{q_2(t)} \tag{4.5}$$

$$\sigma^2{}_1(t) = \sum_{i=1}^{t} [i - \mu_1(t)]^2 \ \frac{P(i)}{q_1(t)} \ \square \tag{4.6}$$

$$\sigma^2{}_2(t) = \sum_{i=t+1}^{I} [i - \mu_2(t)]^2 \ \frac{P(i)}{q_2(t)} \ \square \tag{4.7}$$

t is going to be the threshold. The value of t will range from 0 to 255. P is the probability and $q_1(t)$ and $q_2(t)$ are the probability of class 1 and class 2 respectively. Also μ_1 and μ_2 are the means of class 1 and class 2 respectively. I is the maximum value of image, that is 255.

Once again, this measure, basically, the compactness of the classes. If the threshold is put up in the wrong place then there is going to be a large variance for one of the classes and that is not our optimization condition. So how to find out the value of t such that the optimization function is minimized. One way should just start value of t from zero to 255 and compute for individual values. The value which gives minimum value from all should be taken as the threshold.

$$\sigma^2 = \sigma^2{}_w(t) + q_1(t)[1 - q_1(t)][\mu_1(t) - \mu_2(t)]^2 \tag{4.8}$$

In the above equation 4.8, we can see that σ^2 is the total variance of an image. It is a constant value. If we want to minimize the within class variance then the other term (between class variance) after addition sign should be maximized. So this formula also can be used to find the threshold value. So in simple words what can be done is either equation 4.8 can be used to find the value of t such the between class variance should be maximized

and if we use equation 4.1 to equation 4.9 then we have to minimize the mean class variance for finding the threshold value t. If we have a non-uniform background then Otsu is not going to help. Otsu's algorithm is not going to help because we may have a binary distribution. So the above explanation explains us how to do Otsu's algorithm in the whole image. We can also do it in blocks of the image, to try to get rid of the problem with basically a non-uniform background. And then we're going to get a different threshold for every single one of the region. Or if we want, we can actually do what's called a moving window. And then we can, for example, if we want, we can average the thresholds that we get in the overlapping windows. Or we can create a function of the thresholds.

So once we have separated the foreground and the background in the image using Otsu threshold we will proceed with creating the masked image which is required as one of the parameters in the active contour method without edges[47].

4.4 Creating Masked Image

This is fairly a very simple step in which the background pixels are converted to black values as 0 and foreground pixels are converted to white values as 1. It is shown in the following figures 4.12 to figures 4.14. In the following figure, the background color was made red and the foreground pixels were kept as it is for further analysis. So for creating the mask image, the red pixels were converted to black color i.e. value 0 and the rest pixels intensity were converted to value while color i.e. value 1. The background was made red for better understanding as X-Ray images won’t be having red color in it after converting to grayscale.

Figure 4. 12 Grayscale X-Ray Image

Figure 4. 13 Background Removed Image using Otsu method

Figure 4. 14 Mask Image

4.5 Active Contour method without edges

Here now to find an exact bone part we are using Active contour method without edges[47] with a slight modification in it such that bone portion is easily found out in a maximum number of cases for our work of medical imaging in case of X-Rays especially for long bone structure. This algorithm can be applied to different bones other than long bones also but certain modifications are to be done for that also which is not included in our scope of the study. To understand active contour method we have to get familiar with the concept of different things as explained below. Also, it can start from the curve inside or outside the region boundary and it will expand or deform accordingly until we get the edge boundary in the image.

4.5.1 Signed Distance Map

Firstly we have to calculate the Signed Distance Map (SDF) for the given image matrix and it is the Euclidean distance[55] between the first non-zero pixel and the pixel value. It can be calculated as follows for one of the examples.

Table 4. 2 Table Showing Calculation of Distance Transform

Code	`bw = zeros(6,6);`
	`bw(2,2) = 1;`
	`bw(4,4) = 1;`
	`bw(6,6) = 1`

Calculate Distance transform	`[D,IDX] = bwdist(bw)`
Original Matrix	bw = 0 0 0 0 0 0 0 1 0 0 0 0 0 0 0 0 0 0 0 0 0 1 0 0 0 0 0 0 0 0 0 0 0 0 0 1
Distance Matrix	D = 6×6 single matrix 1.4142 1.0000 1.4142 2.2361 3.1623 3.6056 1.0000 0 1.0000 2.0000 2.2361 2.8284 1.4142 1.0000 1.4142 1.0000 1.4142 2.2361 2.2361 2.0000 1.0000 0 1.0000 2.0000 3.1623 2.2361 1.4142 1.0000 1.4142 1.0000 3.6056 2.8284 2.2361 2.0000 1.0000 0
IDX is Values representing nearest non-zero pixel values	IDX = 6×6 uint32 matrix 8 8 8 8 8 22 8 8 8 8 22 22 8 8 8 22 22 22 8 8 22 22 22 22 8 22 22 22 22 36 22 22 22 22 36 36

Now once we know how to find the signed distance map we want to look about basics of the curve because algorithm of active contour starts with a random curve and then the curve either expand or deform according to our region or edge. We also want to know what is tangent or normal to a curve such that the concept of the level set which is introduced later is understood easily.

4.5.2 Planar Curves

A curve on the plane will define a coordinate system. Here in the figure 4.15, we have a curve parameterized by p. The value of p runs between zero and one. For every other value of p, we get a point on the curve.

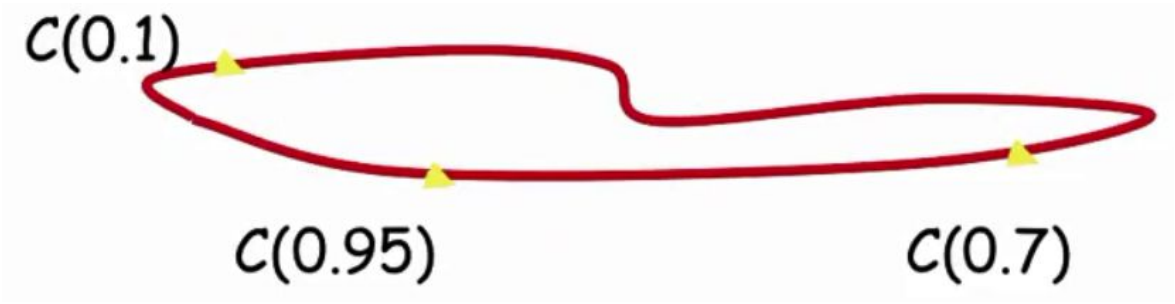

Figure 4. 15 Simple Planar Curve

So, basically, for example, for p equals 0.1, p equals 0.7 and 0.95 points are plotted on the curve using the below-given equation 4.9.

$$C(p) = \{x(p), y(p)\} \; where \; p \in [0,1] \tag{4.9}$$

Now, if a curve is closed like in the above figure we can say that c(0)=c(1). Now let us understand the other couple of concepts like normal and tangent to the curve. So if we find a partial derivative to a function of the curve then it will give the tangent and its perpendicular will be called normal.

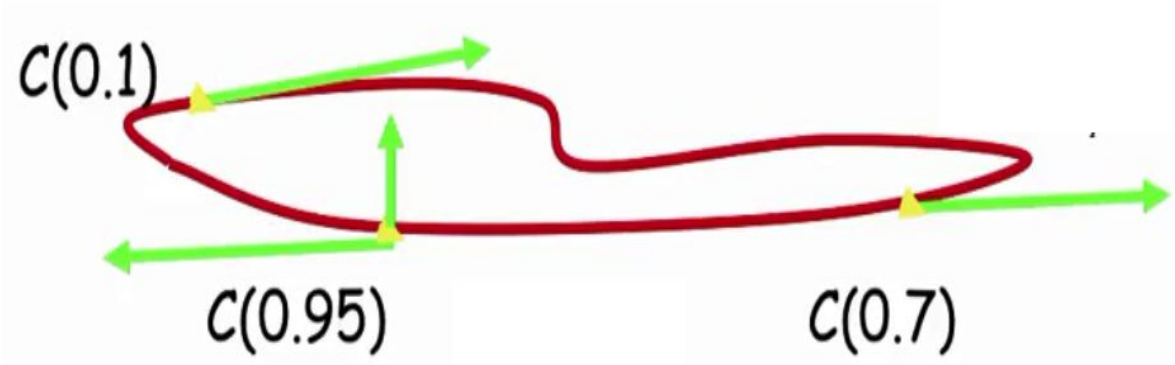

Figure 4. 16 Curve Showing Tangent and Normal

Here in the above figure, we can see in green lines at the different point the tangent to a curve and its perpendicular at point p=0.95 it is normal. The equation of the tangent is as mentioned below. Tangent is a unit vector whereas normal does not have to be a unit vector.

$$\vec{t} = \frac{C_p}{|C_p|} = C_s \tag{4.10}$$

$$Where \; \vec{t} \; is \; tangent, C_p = \frac{\partial C}{\partial p} \; and \; |C_p| \; is \; the \; normal \; length$$

If we find the second partial derivative i.e. C_{ss} we get the normal to that vector. So the

equation of it is

$$C_{ss} = k\vec{n} \tag{4.11}$$

$Where\ k = kapa\ is\ the\ curvature\ and\ \vec{n}\ is\ the\ normal.$

So this is the second derivative. And we call the magnitude of that second derivative we call the curvature. Curvature basically tells us how much the tangent is changing and it's very intuitive. If it changes a lot, it means that the curve is curving along and has very high curvature. If it's not curving a lot, for example, a straight line has zero curvature.

The primary reason to learn the above-mentioned theory is to get a clear idea about what a curve is mathematically and how we can proceed for selecting the next curve to the existing curve using the concept of normal.

Once we know about tangent and normal to the curve and also the curve we can now look at how the curve is evolved.

4.5.3 Curve Evolution

As shown in the following figure 4.17 we can see a curve and that every point on a curve we have a velocity that defines how that curve is moving, and that's represented by the following equation.

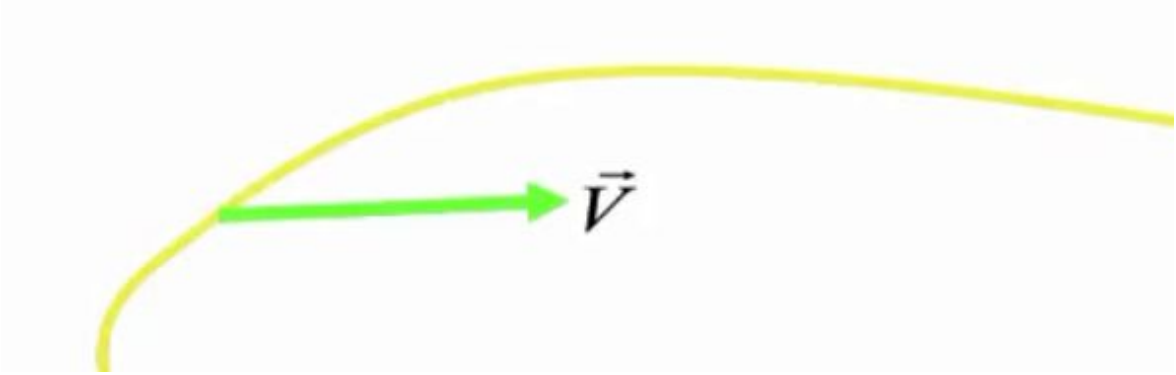

Figure 4. 17 Curve and Velocity

$$C_t = \vec{V} \tag{4.12}$$

$$\frac{\partial C_{lp}}{\partial t} = \vec{V}(p,t) \tag{4.13}$$

Here C_t is the curve and $\vec{V}$ is the velocity. So it's a partial differential equation. So the curve is changing in time, is equal to certain velocity. And the velocity is again, at the given point. And the velocity might be changing in time.

As you can see in the following figure 4.18 we can see that the curve has velocity, tangent and normal to the curve. As we can see that curve does not deform in the tangent direction but it deforms in the normal direction. So it gives rise to an important property that tangential components does not affect the geometry of the curve.

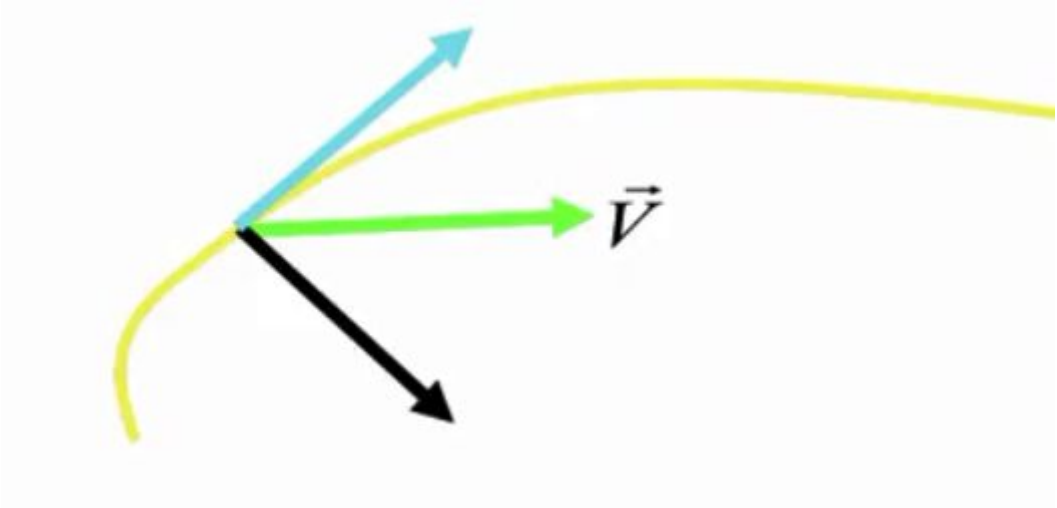

Figure 4. 18 Velocity, Tangent, Normal to Curve

Once we know how the curve evolution is done now we should see the concept of the level set which is the most important part to understand for finding the edge of the object in the image by evolving the curve.

4.5.4 Level Set

In the above topic, it was discussed how the curve evolution works but we have not specified how it can be implemented in the computer. And we need to learn, how we implement in that friendly fashion that in a computer when we have discrete images. So, we need to talk about the numerical implementation of that. One of the areas that have had a tremendous impact in image processing, in particular, when we talk about PDE (Partial Differential Equation) in image processing, is level sets methods and it is explained now. And with that, we are going to know how we implement any type of curve or surface evolution in a computer.

The curve can be geometrically represented as shown in the following equation 4.14

$$C = \{(x, y) | \emptyset(x, y) = 0\} \quad (4.14)$$

It is shown in the below-given figure 4.19 that any point on the curve is equal to zero and if it is the positive value of $\emptyset(x, y) > 0$ it is the point inside the curve and if it is negative $\emptyset(x, y) < 0$ then that point is outside the curve.

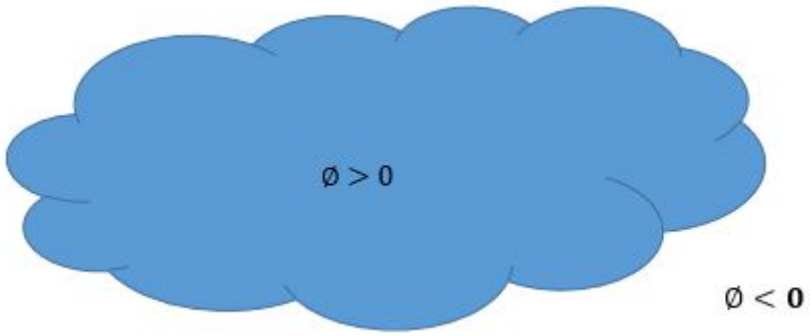

Figure 4. 19 Representation of level Set

And for example, we can define the function to be positive inside and negative outside and one example is to define this as the distance to the curve for, for of course the distance to the curve at the curve itself is zero. The distance to the point itself is zero. So, every point on the curve has zero distance to the curve. Every point inside has a positive distance, and we define every point outside to be at a negative distance. And that way, we define the function phi. That the zero set, that's called the zero level set of that function, meaning all the points in the plain where that function is zero define a curve.

With this representation, we have computed to tangents, normal and curvature. We need to be able to compute it with this representation, otherwise, we won't be able to do curve evolution.

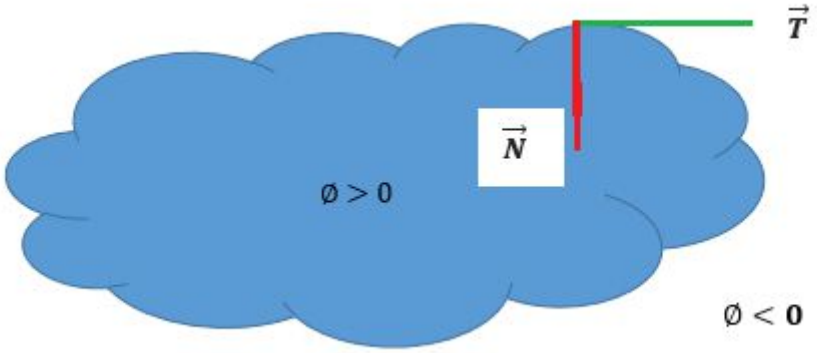

Figure 4. 20 Level Set with tangent and Normal

As shown in the above figure 4.20 we can see that tangent and normal are drawn to the curve. Now the equation of Normal and Tangent to the curve are as follows.

$$\vec{N} = -\frac{\nabla \emptyset}{|\nabla \emptyset|} \tag{4.15}$$

$$\vec{T} = \frac{\bar{\nabla} \emptyset}{|\nabla \emptyset|} \tag{4.16}$$

Here in the above equation 4.15 and 4.16, the numerator is the gradient of phi and the denominator is the magnitude of phi. Equation 4.15 is of normal and Equation 4.16 is off tangent. Now the level set curvature is the defined as the second derivative

$$C_{ss} = k\vec{n} \tag{4.17}$$

$Where\ k = kapa\ is\ the\ curvature\ and\ \vec{n}\ is\ the\ normal.$

$$k = div\left(\frac{\nabla \emptyset}{|\nabla \emptyset|}\right) \tag{4.18}$$

Where div is the divergence and it can be defined as

$$div(\alpha, \beta) = \alpha_x + \beta_y \tag{4.19}$$

Here α_x and β_y are the first partial derivative with respect to x and y respectively. So now if we know the value of $\emptyset$ we can calculate the curvature and tangent and normal to the curve. The value of $\emptyset$ is the signed distance map that we have calculated above. So the next step we have to see that how we can deform the curve such that it find out the shape boundary that is our major interest concern.

Now according to Osher-Sethian[46], [56] we can go for finding the function of the deformation of the curve. How to deform phi in such a way that the boundary, basically, is deforming as we wanted. So, we have a function that is representing a curve in implicit form.

$$C = \{(x, y): \emptyset(x, y) = 0\} \tag{4.20}$$

We know that the curve that is defined in this way, it's moving with the velocity given in equation (4.21).

$$\frac{dc}{dt} = V\vec{N} \tag{4.21}$$

Now the question is how we have to change phi for the level set of phi to move according to the above-given velocity. It is given in equation (4.22) below.

$$\emptyset_t = V|\nabla\emptyset| \tag{4.22}|$$

The phi is once again, it lives on the image. It lives on the grid. Every time I'm talking about derivatives, I'm talking about derivatives on the grid. So the pixels are moving up or down. There are no derivatives on the curve which are very difficult to implement. We get that when we want to move a curve according to V in the normal direction. That's obtained by moving phi up and down, whatever equation 4.22 tells us and then we cut. So you want to go for t equal five, do this for t equal five, find the zero level set and you got the curve evolution. So everything now is in implicit form. We have functions defined on the plane and by moving those functions, we are moving the zero level set and we are getting curve evolution, for example, we are getting active contours.

So level set is quite important for deforming a curve or expanding a curve as explained above and as they can handle change in topology easily they are widely used in medical imaging for evolving a curve.

4.6 Finding the ROI

Once we get the bone part of the image according to the previous step of active contour algorithm will go for finding ROI (region of interest) from that as follows.

The image that algorithm will get from the above step will be having two-pixel values white and black. 1 represents the bone part and 0 will represent the background part.

Purpose of this step is to minimize the working time of the algorithm which leads to minimum time utilization. Using Column wise color segmentation method algorithm separate the bone pixels of the image and also track the starting location of the bone part. Algorithm work as follows

If the column contains a single white pixel then copy the entire column to the new segmented image.

The reason for storing segmentation location is that in future if algorithm wants to restore the image then it will be helpful. All the column which do not contain any white pixels is eliminated from the resultant image. This is how the algorithm will copy the bone part of the image into another image for further processing on it.

The region of Interest (ROI) detection algorithm would mainly focus on the gap between two broken parts of the bone. Here in this step algorithm find the gap using BWB (Black White Black) region detector. BWB region detector detects all those regions where black, white and black region occurs inline. It will scan the entire image column wise and check next 20 pixels to find the occurrence of the BWB region. If this type of region is found then the algorithm will duplicate entire row of this image to a new image and repeat the same till the end.

4.7 Fracture type Detection from ROI

After detecting the ROI algorithm measure the number of pixels each ROI will contain and based on that crack measurement will be done. As mentioned below for one of the instances of the different crack type, algorithm select appropriate crack type for each ROI region.

Based on the size of the fracture/crack algorithm will divide them into 3 categories:

1. Hair-line crack
2. Minor crack
3. Major crack

4.8 Annotating Original Image according to ROI

Now the region of interest (ROI) was detected and the measurement was also taken automatically, algorithm restore back all the ROI and measurement to the original image. In finding the ROI step algorithm store the starting location of the segmentation, using that location we restore the ROI region to the image also superimpose/annotate the crack type as a text box on the image.

In this step, algorithm fetches the appropriate surgical diagnosis from the database and displayed to the user/doctor. Measurement taken in the ROI detection steps are used here, the algorithm checks the pixels size of each region and based on that algorithm fetch the appropriate diagnosis.

Diagnosis database is loaded into the algorithm when it starts. At the starting point, if the diagnosis database is not available the user/doctor have to create one database of diagnosis. The algorithm provides the utility to create a database so that doctors can easily create diagnosis database. Once the database is created, now whenever algorithm is executed user have to load that database.

CHAPTER – 5

Design and Development of System for Automatic Identification of ROI in Bone Images

5.1 Introduction

This chapter is all about the algorithm, flowchart, and system layout of the application developed for testing up of the automatic identification of the region of interest in bone images. Firstly algorithm is described in detail followed by a flowchart as another topic. Various screen layout required for automatic identification of the region of interest in bone images are given in a later part in this chapter.

5.2 Algorithm (ROIMI)

[EXECUTE THE SYSTEM(Region of Interest in Medical Imaging-ROIMI)]

Go to app directory and run ROIMI.

1. [LOAD X-RAY IMAGE]

1.1. [LOAD DIAGNOSIS DATABASE]

1.1.1. IF [Database in not Available or not created] then

1.1.1.1. Run diagnosis management system

1.1.1.1.1. Input diagnosis information system

1.1.1.1.2. Add diagnosis by pressing “ADD” button.

1.1.1.2. Exit

1.1.2. ELSE [go to diagnosis database directory]

1.1.2.1. Select database

1.1.2.2. load the database by pressing “Load” button

1.2. [LOAD X-RAY IMAGE]

1.2.1. The user will go to image directory and select x-ray image. (Here ROIMI take three image format as input ‘.jpg’, ‘.png’ and ‘.bmp’)

1.2.2. IF [image type is not appropriate] then ROIMI will generate an error.

2. [GRAYSCALE CONVERSION]

2.1. IF [loaded image is RGB] then

2.1.1. ROIMI convert the loaded image into a grayscale image

2.2. ELSE [keep it as Grayscale image]

2.3. ROIMI also generate empty result image Resultant image is as similar as the source image.

3. [BACKGROUND REMOVAL]

3.1. Perform automatic thresholding to find the threshold for segmenting background. The algorithm calculates Multi threshold (7 thresholds) from the image using Otsu’s method and the select first threshold for background segmentation.

3.2. The algorithm performs COLUMN wise segmentation with a selected threshold and separate background and foreground pixels of the image, then it creates a new segmented RGB image and makes background pixel value as “RED” and others are as it is. From now segmented image is used as the source image.

4. [MASK GENERATION]

The algorithm uses active contour method for bone detection, this method requires two images as input first one is source image and the second one is mask image. The algorithm will create mask image (Here mask image is a Black and white image).

4.1. The algorithm performs COLUMN wise separation on the segmented image and makes background pixel (RED pixel) as 0 and foreground pixels as 1 as follows.

4.1.1. Repeat Iteratively for all rows and columns such that IF [Segmented image (row, column) is equal to “RED”] then make Mask image as 0 else make it 1

5. [BONE DETECTION] Using Active contour method

5.1. To reduce the time taken by this method algorithm will Resize the image by half as follows

5.1.1. Algorithm resizes the source image as well as mask image by half. MATLAB provides the built-in function 'imresize(source-image, scale)' which takes source-image and resize scale as input and returns output image that is scale times the size of source-image.

5.2. [ACTIVE CONTOUR METHOD]

5.2.1. Call active contour method and pass source-image and mask image as input

5.2.2. [GRAYSCALE AND TYPE CONVERSION]

5.2.2.1. IF[source-image is not grayscale] then

Convert image to grayscale image

5.2.2.2. Convert image type to double

5.2.3. [SIGNED DISTANCE MAP(SDF)]

5.2.3.1. Using 'bwdist(image)' MATLAB function algorithm computes the SDF from the mask image and named as 'phi'

5.2.4. [BONE DETECTION LOOP]

[Declaration]

its=1;

its= iterations

dupits= duplicate iterations

breakrange=20;

prevC1=0.0;

c1=0.0;

const=20;

5.2.4.1. While dupits is less than or equals to break-range

5.2.4.1.1. Find the narrowband curve (called 'idx') of the phi

IF phi(pixel) is less than or equals to 1.2 and greater than and equals to -1.2 then

Add phi(pixel) to idx

[Exit IF]

5.2.4.1.2. Find the interior point(called 'upts') of the phi

IF phi(pixel) is less than or equals to 0 then

Add phi(pixel) to upts

5.2.4.1.3. Find the exterior point(called 'vpts') of the phi

IF phi(pixel) is greater than 0 then

Add phi(pixel) to vpts

5.2.4.1.4. The store previously calculated constant c1 and then Calculate the two constant c1 and c2 as a mean of the interior and exterior pixels for the source image (named "I") respectively.

```
prevc1 = c1;
c1 = (sum(I(upts))/(length(upts)+eps))+20; % interior mean
c2 = (sum(I(vpts))/(length(vpts)+eps)); % exterior mean
```

5.2.4.1.5. Calculate the force for moving the curve either inside or outside the object force F = square of curve value of source image minus constant c1 minus square of curve value of source image minus constant c2 as follows:

$$F = (I(idx)-c1)^2 - (I(idx)-c2)^2$$

5.2.4.1.6. [CURVATURE CALCULATION]

5.2.4.1.6.1. Get the subscripts of the curve indices

5.2.4.1.6.2. Calculate four direction neighbors

5.2.4.1.6.3. Get the 8 neighbors for all the pixels and calculate indices

5.2.4.1.6.4. Calculate the central derivatives of SDF (phi) for every pixel

5.2.4.1.6.5. Now using central derivatives of the phi calculate the curvature

5.2.4.1.7. [ENERGY MINIMIZOR]

5.2.4.1.7.1. Now based on the force and curvature algorithm calculate the new gradient descent to minimize the energy of the image

5.2.4.1.8. Maintain the CFL (Courant Friedrichs Lewy) condition by dividing maximum force of the source image from the decided constant (here constant is 0.45)

```
dt = .45/(max(dphidt)+eps);
```

5.2.4.1.9. [CURVE EVOLUTION]

5.2.4.1.9.1. By the addition of the product of the CFL (Courant Friedrichs Lewy) and gradient decent energy minimizer algorithm evolve new curve for the object.

5.2.4.1.10. [To keep the SDF smooth algorithm use Sussman method]

Level set re-initialization by the Sussman method

5.2.4.1.10.1. First, algorithm calculate the forward/backward differences of new SDF (or also called 'phi')

5.2.4.1.10.2. Second, find the negative and positive differences

5.2.4.1.10.3. Third, IF the positive difference is less than 0 then make it 0 same as IF negative difference is greater than 0 then make it 0

5.2.4.1.10.4. Forth, find the negative and positive indices of the SDF

5.2.4.1.10.5. Fifth, based on positive and negative indices algorithm calculates the difference between positive and negative indices

5.2.4.1.10.6. Sixth, using Sussman sign function algorithm finally smooth the new phi

5.2.4.1.11. [LOOP BREAKING CONDITION]

5.2.4.1.11.1. Calculate the difference between previous c1 and current c1

IF the difference is similar to the previous loop then

IF dupits is less than or equals to break range then

Increment the dupits by 1

ELSE

Break the loop

[END IF]

ELSE

Reset the dupits

[END IF]

5.2.4.1.11.2. IF iterations equal to max iterations

Break the loop

[END IF]

5.2.5. Display the segmented bone image

6. [BONE EXTRACTION]

6.1. From the segmented bone image algorithm extract the bone part of that image and remove unnecessary image data

6.2. By performing color-based COLUMN wise segmentation on black and white image algorithm eliminates the unnecessary black pixels of the image

6.3. Algorithm also store the bone starting position to restore the removed part of the image in future

7. [ROI DETECTION]

7.1. The algorithm generates empty image same size as the segmented image and named it a region of interest image.

7.2. For each column in the segmented image

7.2.1. Find out white pixels and look forward for 20 pixels

7.2.1.1. IF black pixels come in between white pixels

7.2.1.2. Algorithm mark that entire row as ROI and store it in the region of interest image.

7.2.2. Repeat the process until all the column are visited

7.3. [FRACTURE MEASUREMENT]

7.3.1. Now, for each row in the region of interest image

7.3.1.1. The algorithm finds the white block in the region of interest image and stores the location of that block into a vector of fracture.

7.3.1.2. And algorithm measure the size of each block

8. [IMAGE RESTORATION]

8.1. Now algorithm tracks the location of blocks of fracture and restores that blocks on the resultant image using the starting location of ROI. And

8.2. Using blocks of fracture new location algorithm superimpose crack type (like a hairline crack, minor crack, major crack) and make that blocks as red.

9. [Diagnosis]

9.1. As per the crack found in the image algorithm fetch the diagnosis from the Diagnosis database and displayed to the operator.

5.3 Algorithm Explanation

Input

X-ray machine captures the x-ray of human bone and patched it on the metallic plate. Nowadays, there are a variety of machine/ devices available in the market to scan the x-ray plate and convert it into DICOM/JPEG image. Currently, the algorithm doesn't make any specification regarding the size of the image, so it will take any size of the image as input. Measurement of the crack depends on the number of pixels in which it spread.

Grayscale Converter

Grayscale convertor converts RGB image[52] into a grayscale image by eliminating the hue and saturation information and preserve the luminance.

Background removal

In this step, the algorithm will remove the background portion of the x-ray image. Background partition is unnecessary data for my work. Here algorithm uses Otsu's thresholding method[9] to find the appropriate threshold. The resultant threshold is further used to differentiate the background pixels in the image.

Example of Otsu's multi-threshold is:

Threshold=Multithresh(image, N);

Here, Multithresh[57] method return the N threshold for the source image.

After computing, multiple threshold algorithms used the first threshold to perform column wise threshold segmentation and eliminate the background pixels. Rather than removing those pixels which may lead to unbalancing the image algorithm marked them as background pixels and make their color red.

Column-wise threshold segmentation performs preceding operation:

$$threshold = multithresh(imSRC, 7)(1)$$

$$imBGR(u,v) = \begin{cases} imBGR(u,v,1) = 255, & if\ imSRC(u,v) < threshold \\ imSRC(u,v), & if\ imSRC(u,v) > threshold \end{cases}$$

Here, imSRC is source image imBGR is output image, an image without background.

Mask Generator

To perform active contour method ROIMI requires a starting position of the curve. To assign starting position ROIMI generate mask equivalent to the image without background or in other word x-ray image with bone and soft tissues except for background pixels.

Mask image has the same size as imBGR and ROIMI named it as imMASK. Mask image is a black and white image so to compute the mask image from imBGR ROIMI below

given operation is performed:

$$imMASK(u,v) = \begin{cases} 0, & if\ imBGR(u,v,1) = 255 \\ 1, & if\ imBGR(u,v,1) < 255 \end{cases}$$

This mask image is an important factor for bone detection, therefore, mask generation is a crucial part of the algorithm. Now mask image (imMASK) and removed background image (imBGR) passes to next operation.

Bone Detector

Bone Detector is a heart of the algorithm because here the actual bone is detected from the x-ray image and all the further steps are dependent on the resultant bone of this step. To detect bone from x-ray image ROIMI uses and modify the method/algorithm "Active contour without Edges" developed by Tony F. Chan and Luminita A. Vese[47]. The algorithm takes two input image one is source image and another is mask image (initial curve) and performs below-given steps to detect bone:

1. GRAYSCALE AND TYPE CONVERSION:
   1. IF [source-image is not grayscale] then convert the image into a grayscale image
   2. Convert image type to double
2. SIGNED DISTANCE MAP(SDF): Using 'bwdist(image)'[55] MATLAB function ROIMI compute the SDF from the mask image and named as 'phi'
3. BONE DETECTION: in this step, ROIMI iterate some of the function until ROIMI got the bone
   1. Find the narrow band of the curve
   2. Find interior and exterior point of the curve
   3. Calculate the constant C1 and C2 (mean of interior and exterior point respectively)
   4. Calculate the force for moving curve
   5. Based on the force calculate the curvature
   6. Minimize the energy and calculate gradient descent
   7. Evolve the curve based on curvature, force, and gradient
   8. Smooth the evolved curve

Above algorithm produce the black and white image where 1 represent the bone and 0 represent the background.

Bone Extractor

Purpose of this step is to minimize the working area of the algorithm which leads to minimum time utilization. Using Column wise color segmentation method[58]ROIMI separated the bone pixels of the image and also track the starting location of the bone part. Algorithm work as,

If the column contains a single white pixel then copy the entire column to the new segmented image

The reason for storing segmentation location is that in future if ROIMI wants to restore the image then it will be helpful. All the columns which do not contain any white pixels are eliminated from the resultant image.

ROI Detection

The Region of Interest (ROI)[44] detection algorithm is mainly focused on the gap between two broken part of the bone. Here in this step, ROIMI finds the gap using BWB (Black White Black) region detector. BWB region detector detects all those regions where black, white and black region occurs inline. It will scan the entire image column wise and check next 20 pixels to find the occurrence of the BWB region. If the region found then algorithm make a copy of entire row to the new image and repeat the same process until the end.

After detecting the ROI, ROIMI will measure the number of pixels each ROI will contain and based on that crack measurement will take place.

Image Restoration

Now the region of interest (ROI) was detected and the measurement is also taken, ROIMI will restore back all the ROI and measurement to the original image. In Bone extractor step ROIMI store the starting location of the segmentation, using that location ROIMI restore the ROI region to the image also superimpose the crack type as a text box on the image.

Doctor Diagnosis

In this step, ROIMI will fetch the appropriate surgical diagnosis from the database and displayed to the user/doctor. Measurement taken in the ROI detection steps are used here, ROIMI check the pixels size of each region and based on that ROIMI fetch the appropriate prescription.

Diagnosis database is loaded into the system when it starts. At the starting point, if the diagnosis database is not available the user/doctor will have to create one database of diagnosis. ROIMI provide the utility to create a database so that doctors can easily create diagnosis database. Once the database is created, now whenever ROIMI is executed user have to load that database.

5.4 Flowchart of ROIMI

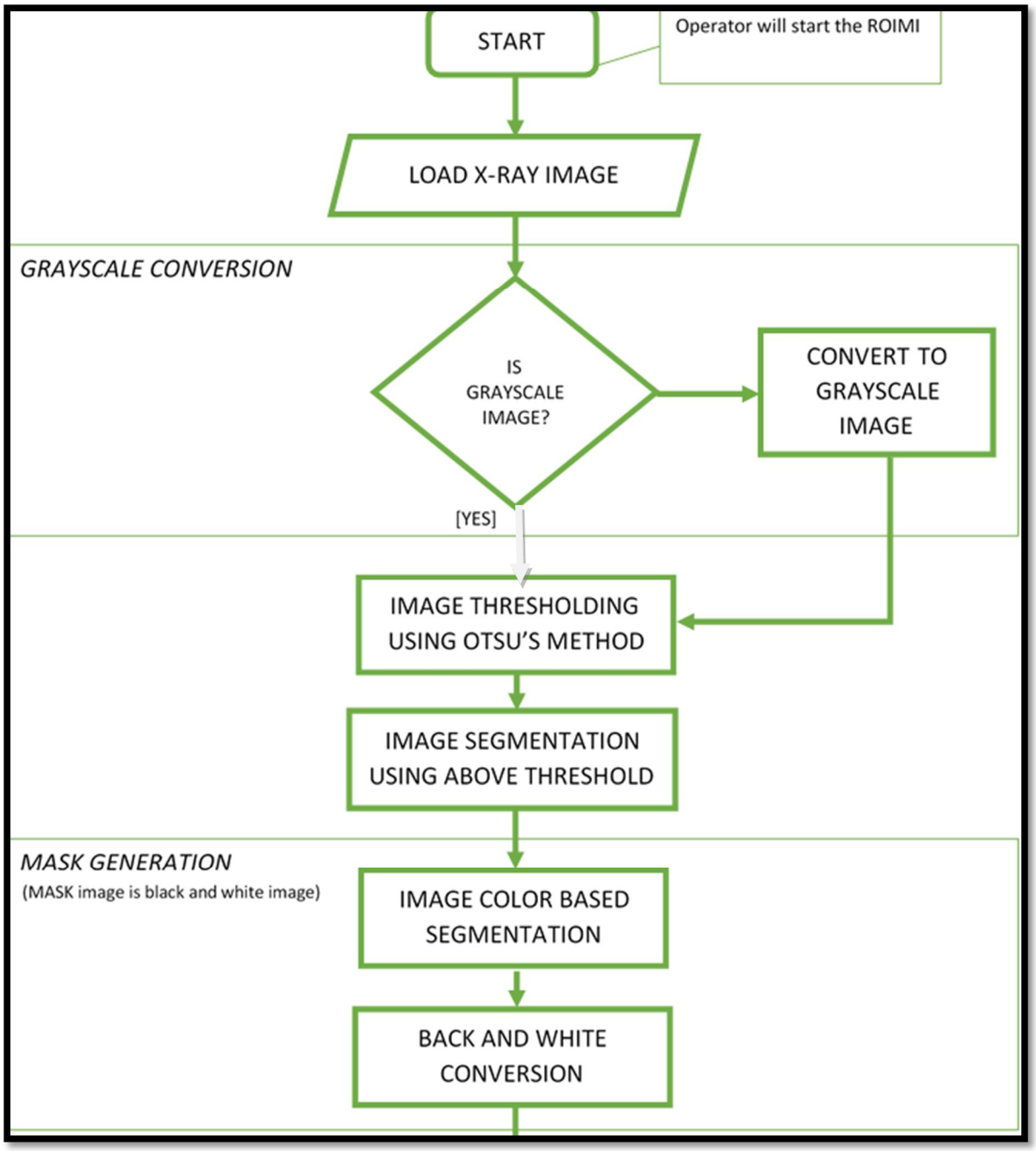

Figure 5. 1 Flowchart-1

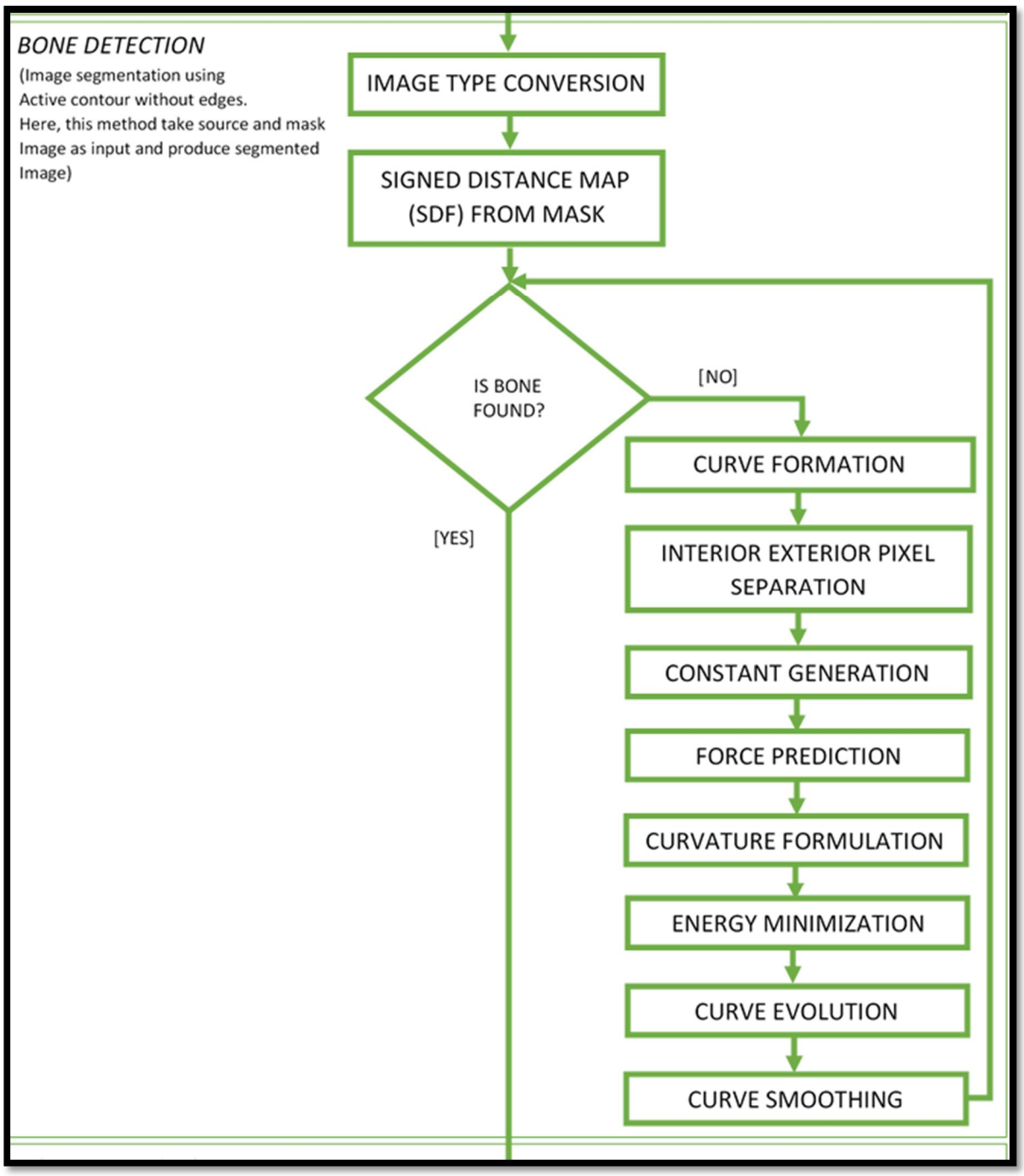

Figure 5. 2 FlowChart-2

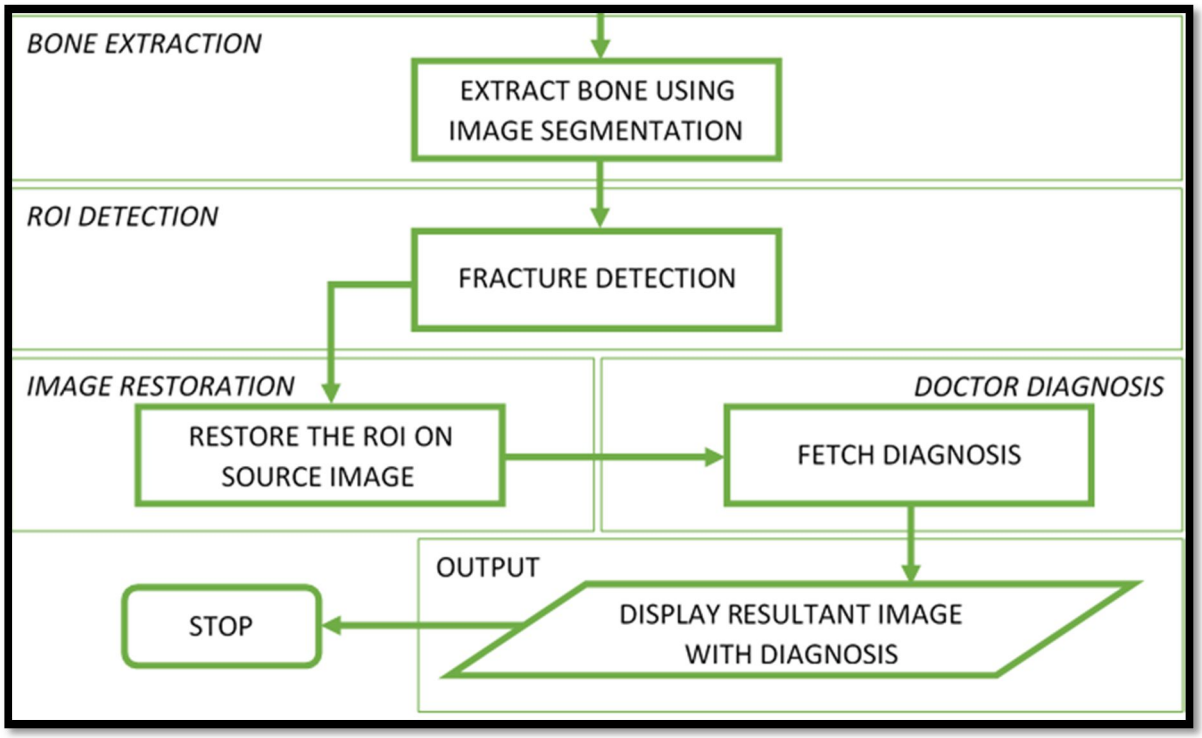

Figure 5. 3 FlowChart-3

5.5 System Layout of ROIMI

ROIMI is a single screen application in which user just have to input the image to the system and all other steps are automated. And if the system is configured with plate scanner then the system automatically takes input from the plate scanner output.

Here, for testing of the algorithm, the system is developed as one testing application which displays every internal step of the algorithm.

Home screen

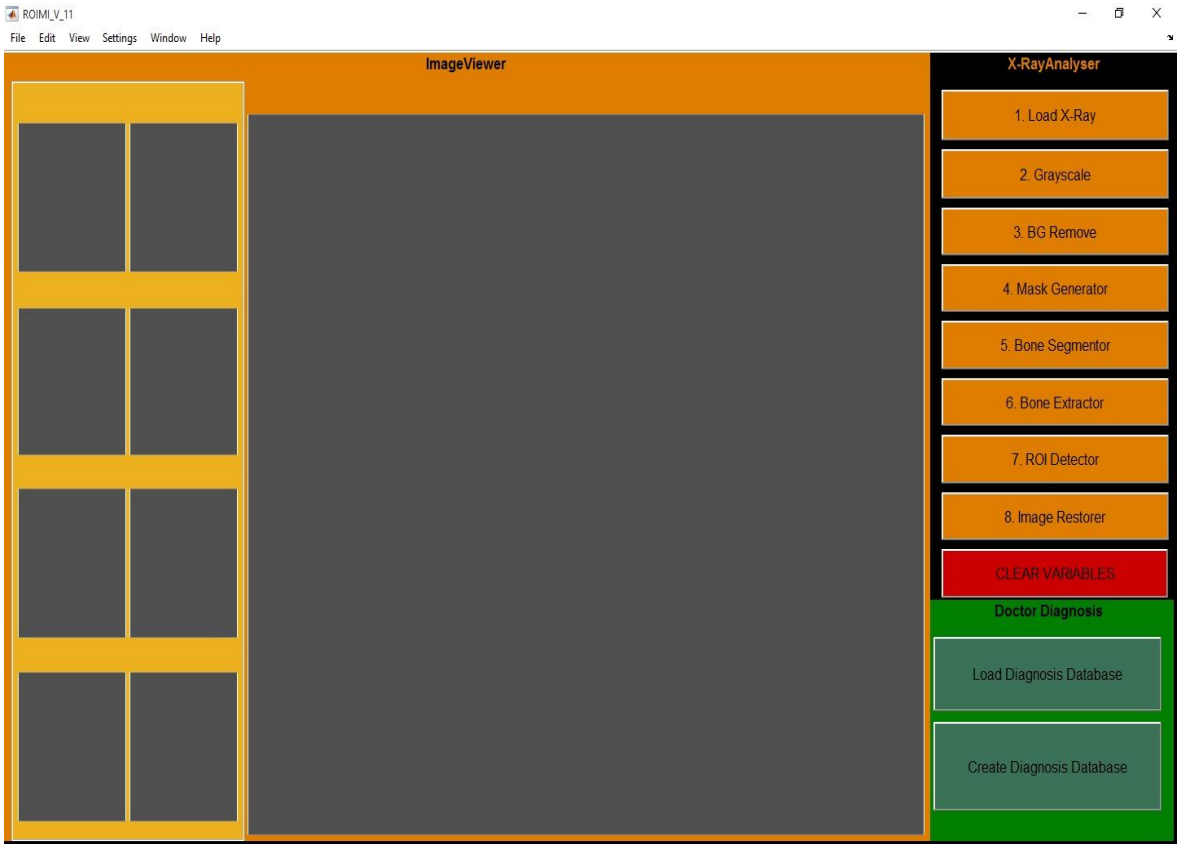

Figure 5. 4 Home Screen

It will display all the menu item of the system. The right panel of the home screen contains menu bar and the menus are:

1) Load X-Ray: menu item used to load the x-ray image.
2) Grayscale: menu item used to call the grayscale converter and convert RGB image to grayscale image.

3) BG Remove: menu item is background remove menu used to call background remover which removes the background.
4) Mask Generator: menu item call mask generator to generate mask.
5) Bone Segmentor: menu item call active contour algorithm and detect the bone
6) Bone Extractor: menu item calls bone extractor to eliminate the unnecessary part of the bone.
7) ROI Detector: menu item call ROI detector which detects ROIs
8) Image Restorer: menu item call image restore to superimpose the ROIs
9) Clear variables: menu item clear all the global variables of the system.
10) Load Diagnosis Database: menu item to load the Diagnosis database.
11) Create Diagnosis Database: menu item creates the diagnosis database.

Load Diagnosis Database

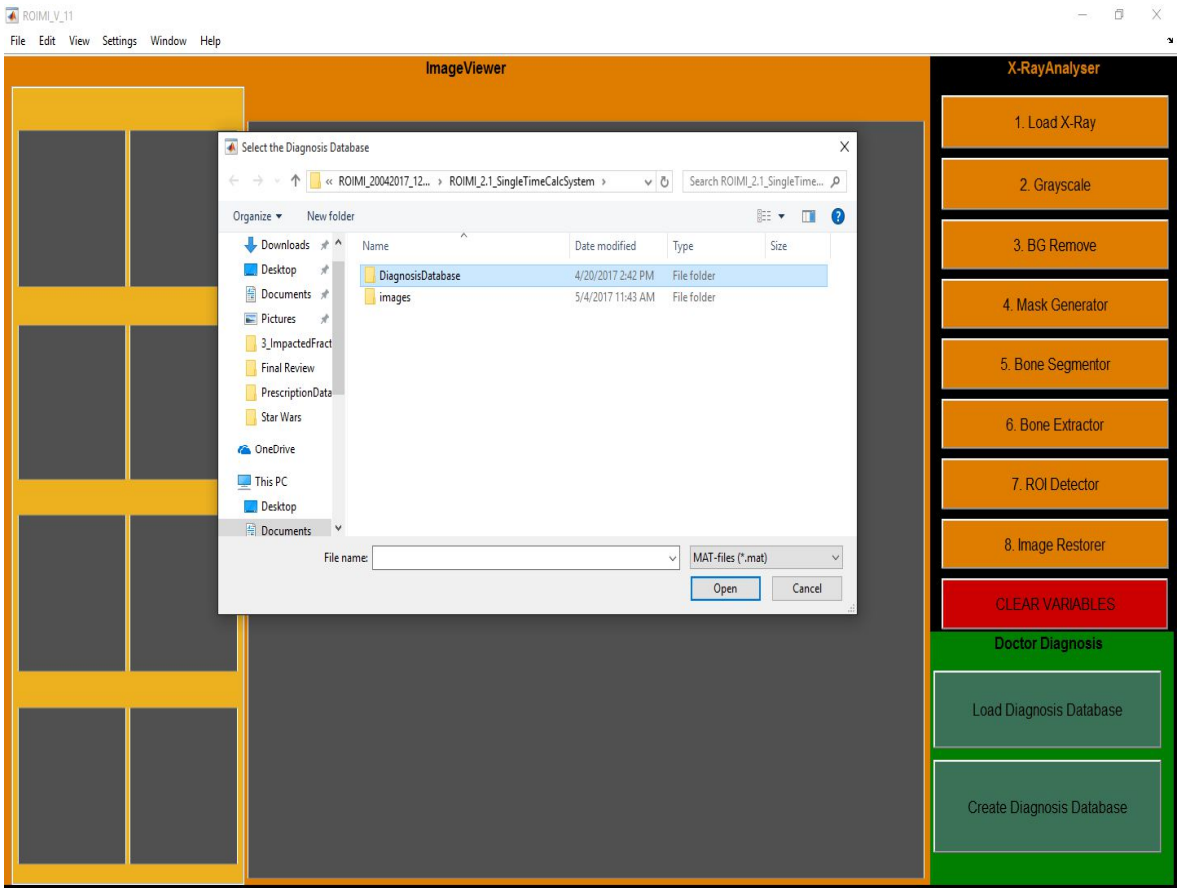

Figure 5. 5 Load Diagnosis Database

User/doctor needs to load diagnosis database at the time of starting the application. Application database store the automatic decision support for the system and also information regarding surgery and therefore it is essential to load into the system.

Input (Load X-ray)

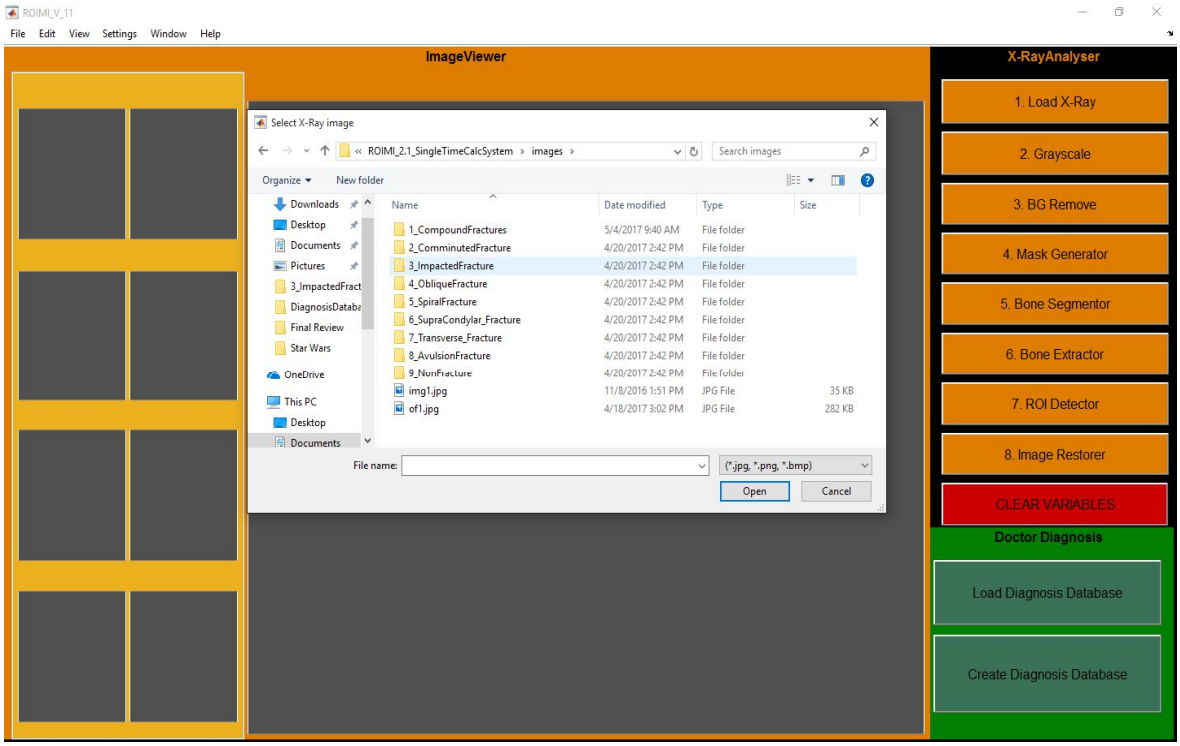

Figure 5. 6 Load X-Ray -1

Now user can execute the application, the user will click on load X-ray menu item and select appropriate x-ray and load into the system.

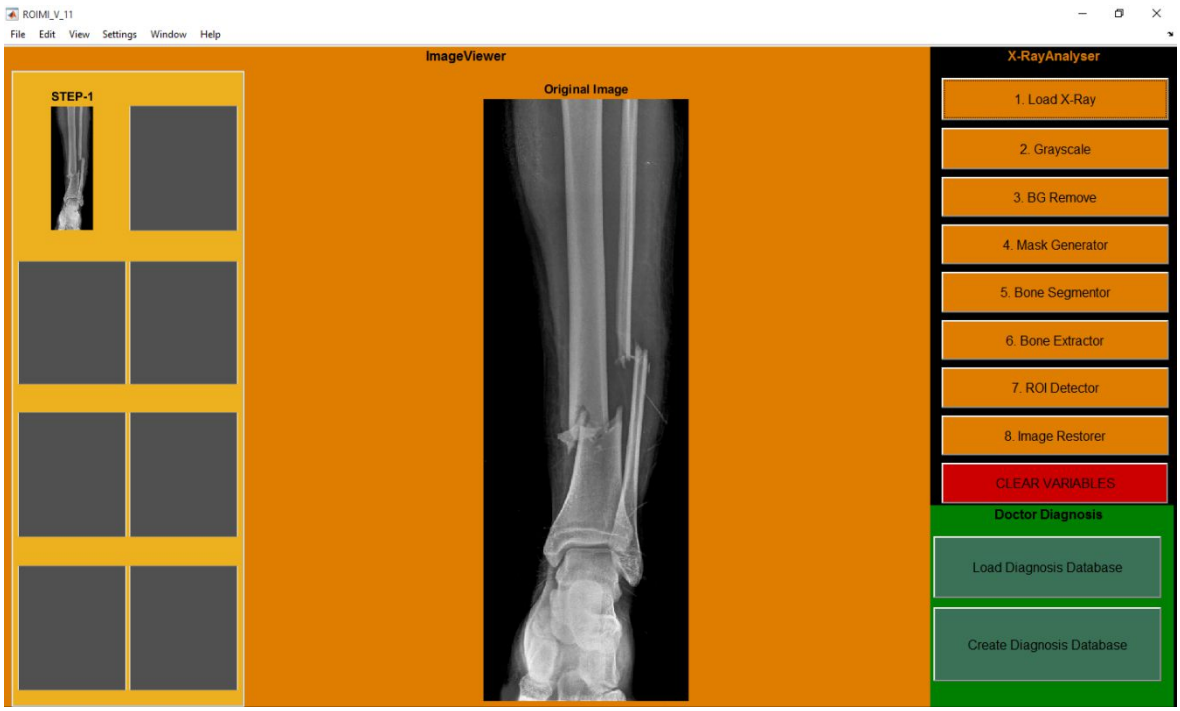

Figure 5. 7 Load X-Ray-2

Grayscale Converter

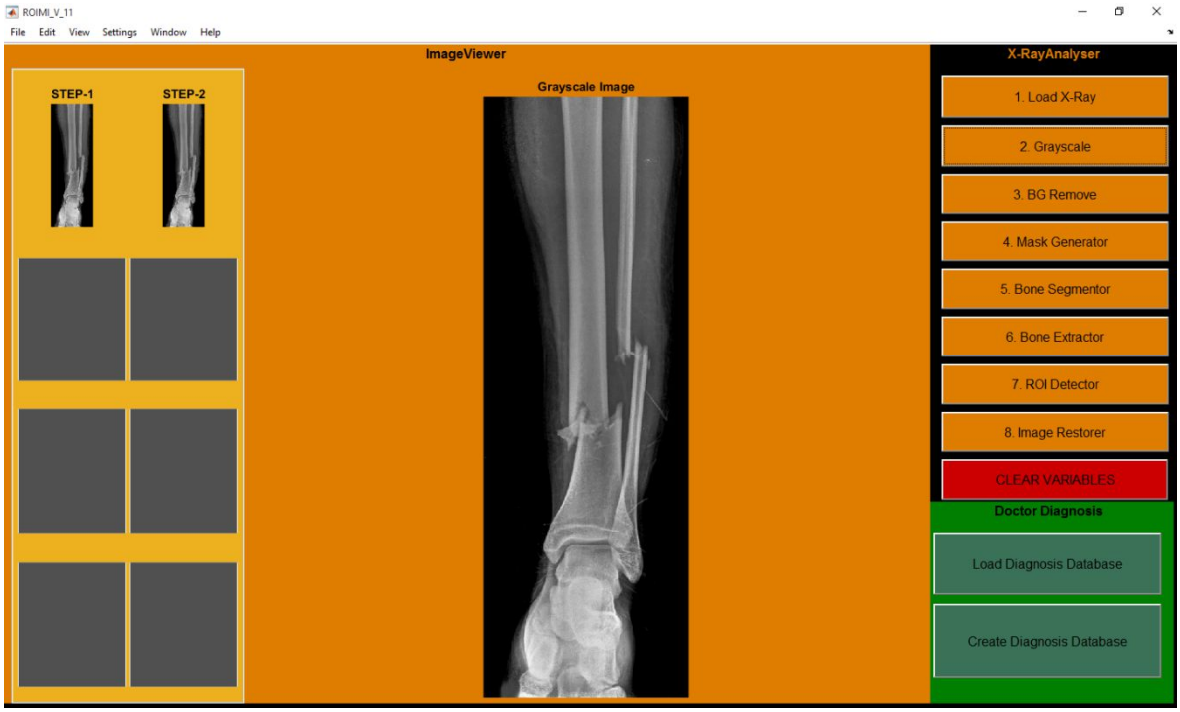

Figure 5. 8 Grayscale Conversion

Grayscale convertor convert RGB image to grayscale.

Background Removal

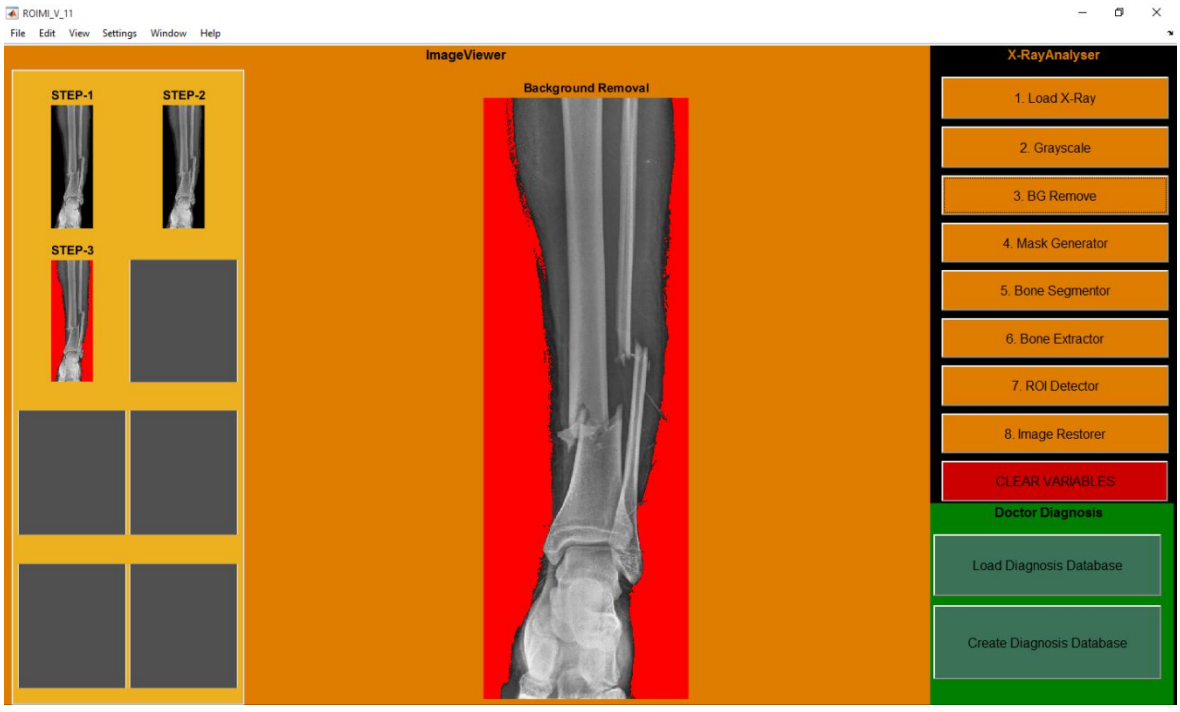

Figure 5. 9 Background Removal

Background remover removes the background of the image and for the demarcating purpose, it is made red.

Mask Generator

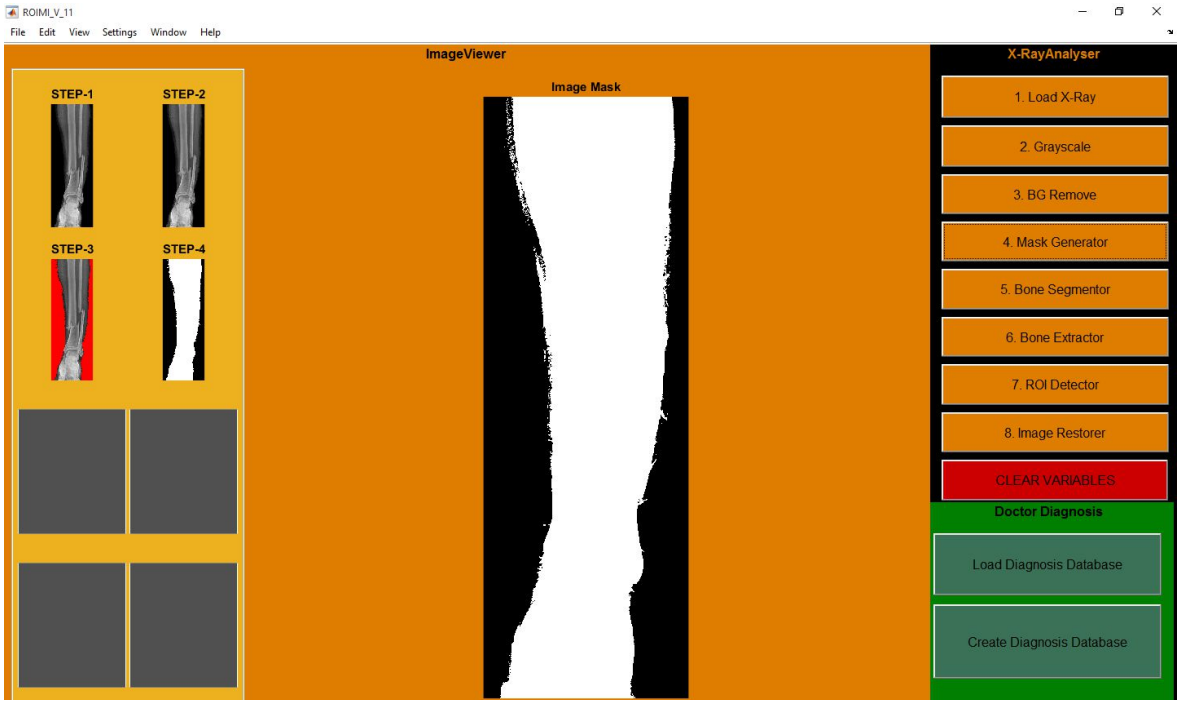

Figure 5. 10 Mask Generator

Mask generator generates a mask for active contour method. Here the white portion represents an active portion of the image (we can call it as “interior points”) and black portion represent a passive portion of the image (exterior points).

Bone Detector

Figure 5. 11 Bone Detector

Bone detector use active contour method and iteratively find the bone portion of the image and at the end make the bone portion as white and others as black. And return the black and white image.

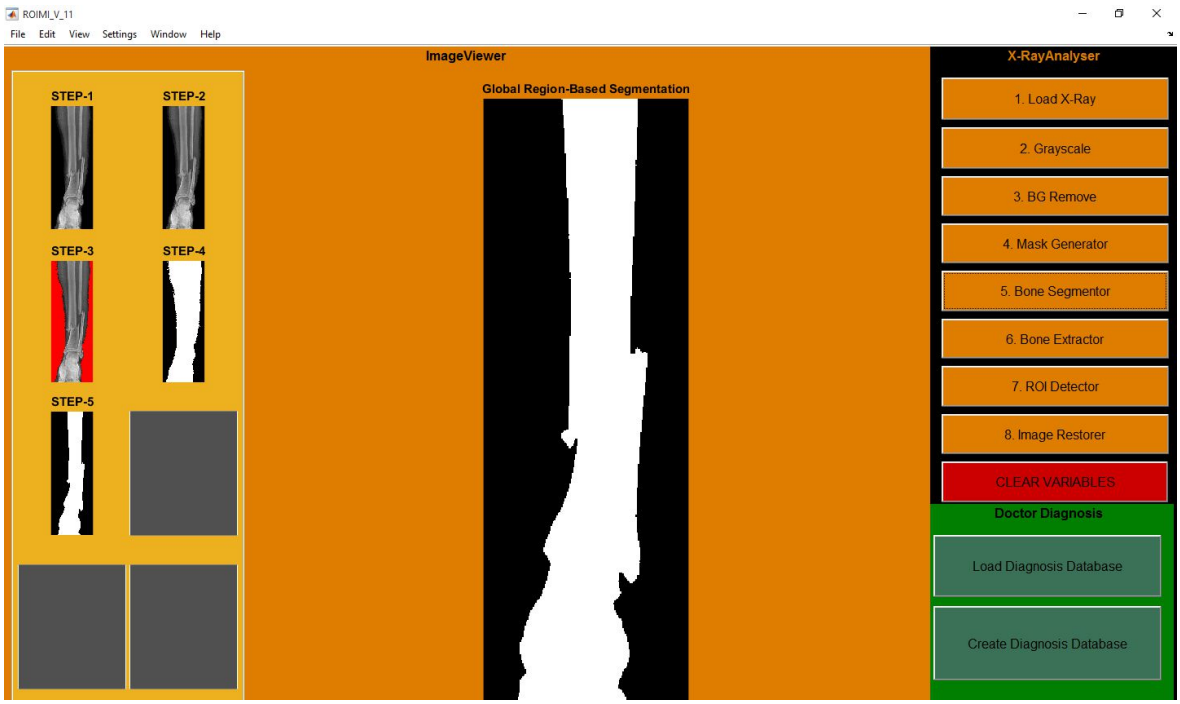

Figure 5. 12 Global Region-Based Segmentation

Bone Extractor

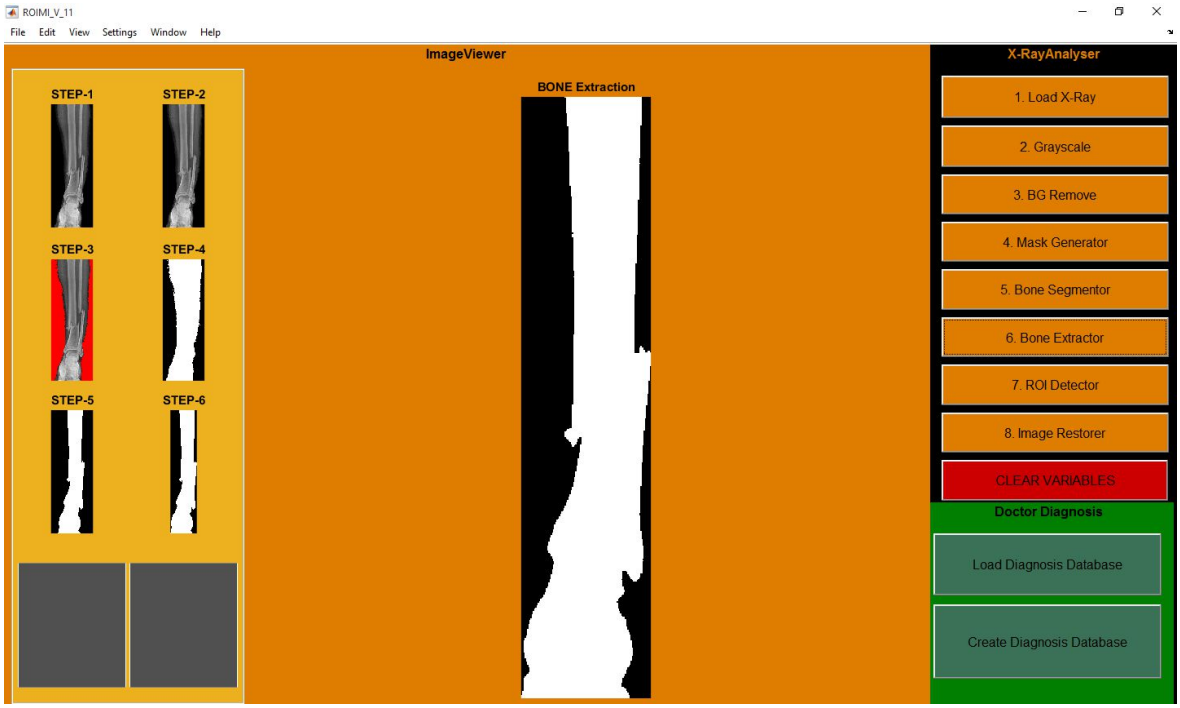

Figure 5. 13 Bone Extractor

To eliminate the extra work, Bone extractor removes the unnecessary data and preserves only bone portion.

ROI Detector

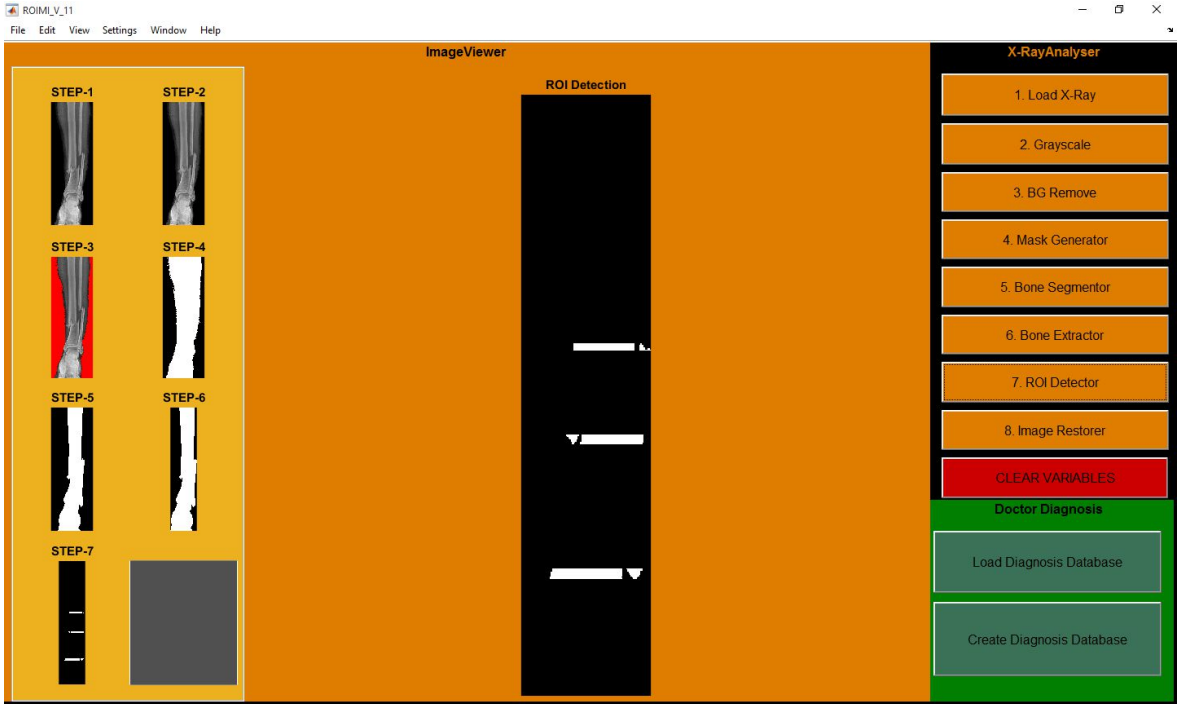

Figure 5. 14 ROI Detector

Using BWB region Detector, ROI Detects crack regions and this steps also measure the ROI regions. All the ROI region location are further used in future steps.

Image Restorer

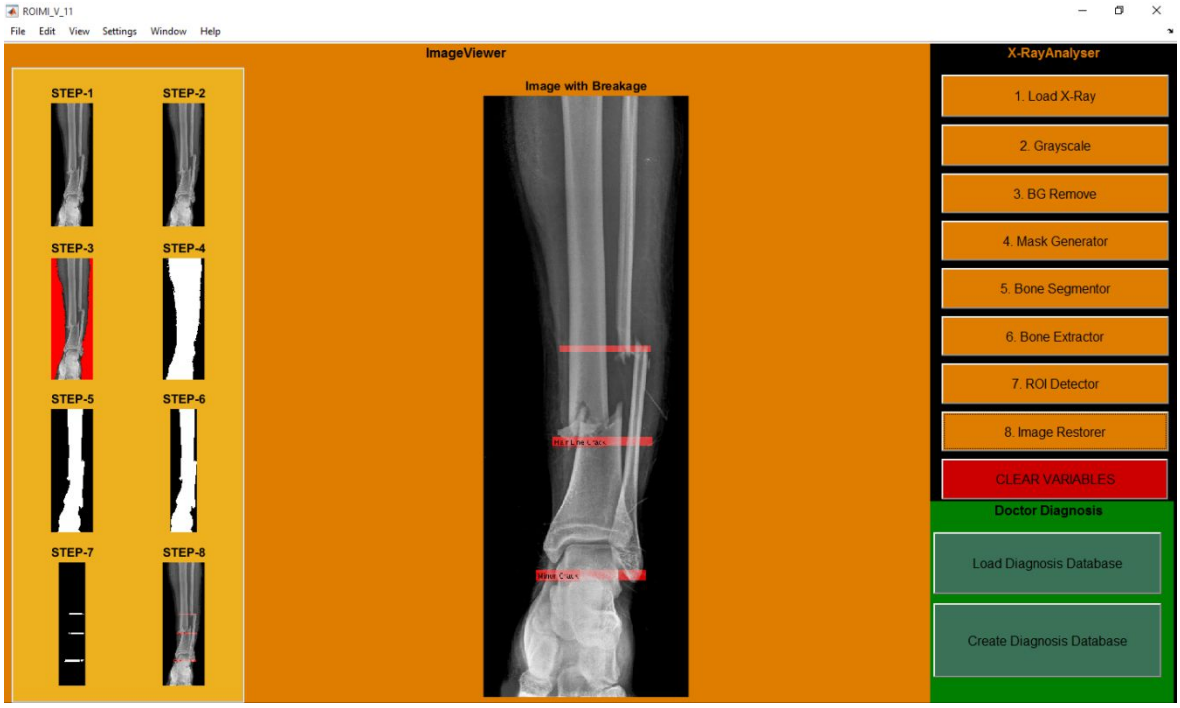

Figure 5. 15 Image Restoration

Image restorer is the last step of the algorithm. It will provide the output of the entire process. Image restorer takes all the ROI regions and their location and superimposes the crack type. It will also fetch the prescription from the database and display to the user.

Surgical Diagnosis Report

ROIMI generate surgical diagnosis steps report. By following that step normal nurse/boy can cure the patient problem or may call the doctor in an emergency situation. The below type of report is generated.

Figure 5. 16 Final Diagnosis / Decision Support

5.6 Conclusion

From the above system, it is clear that algorithm developed is able to find out region of interest in most of the cases along with the surgical diagnosis to be done in that instance. Through this technique, time would be saved and the appropriate decision can be taken very fast such that patient does not suffer much.

CHAPTER - 6:

Results and Discussions

6.1 Introduction

This thesis proposes a decision support system and ROIMI algorithm for automatic detection of bone fracture in the X-Ray image. This chapter presents the simulation results obtained using MATLAB. The results have been obtained by conducting a trial on a dataset of 90 fracture and non- fracture X-Ray images. The dataset comprises of 10 images each for 8 different fracture types and 10 non-fractured images. The system is tested for the time required to produce the resultant image and the percentage of recall.

Results obtained demonstrate the performance of the system for automatic identification of bone fracture in the X-ray image. The results of this novel system are promising, demonstrating that the proposed method is capable of automatically detecting hairline, minor and major type's fractures accurately, and shows potential for clinical application. The results obtained were verified with the doctor for more clarity.

6.2 Results

The following tables display the image of particular fracture type as the input image, the elapsed time to segment bone from the image, identify the type of breakage and annotate the diagnosis based on the size of breakage.

6.2.1 Compound Fracture

Table 6. 1 Compound Fracture-1

Image Name	Description	Output
Of2.png	Input Image	
	Time Elapsed (in Seconds)	8.335972
	Output image	
	Diagnosis	Consult Doctor Immediately

Table 6. 2 Compound Fracture-2

Image Name	Description	Output
Of3.jpg	Input Image	
	Time Elapsed (in Seconds)	26.027611
	Output image	
	Diagnosis	Minor Crack (Plaster Cast, Traction) Major Crack/Supracondylar fracture (External Fixation (Emergency))

Table 6. 3 Compound Fracture-3

Image Name	Description	Output
Of4.jpg	Input Image	
	Time Elapsed (in Seconds)	72.251594

	Output image	
	Diagnosis	Major Crack/Supracondylar fracture (External Fixation (Emergency))

Table 6. 4 Compound Fracture-4

Image Name	**Description**	**Output**
of1.jpg	**Input Image**	
	Time Elapsed (in Seconds)	2.414892
	Output image	
	Diagnosis	Major Crack/Supracondylar fracture (External Fixation (Emergency))

6.2.2 Comminuted Fracture

Table 6. 5 Comminuted Fracture-1

Image Name	Description	Output
CF1.jpg	**Input Image**	
	Time Elapsed (in Seconds)	231.472932
	Output image	
	Diagnosis	Hair Line Crack (Normal Treatment, Take Rest and Don't Move Fractured Part) Minor Crack (Plaster Cast, Traction) Major Crack/Supracondylar fracture (External Fixation (Emergency))

Table 6. 6 Comminuted Fracture-2

Image Name	Description	Output
CF2.jpg	**Input Image**	
	Time Elapsed (in Seconds)	12.492602

	Output image	
	Diagnosis	Minor Crack (Plaster Cast, Traction)

Table 6. 7 Comminuted Fracture-3

Image Name	**Description**	**Output**
CF3.jpg	**Input Image**	
	Time Elapsed (in Seconds)	8.570791
	Output image	
	Diagnosis	Minor Crack (Plaster Cast, Traction)

Table 6. 8 Comminuted Fracture-4

Image Name	Description	Output
CF4.jpg	**Input Image**	
	Time Elapsed (in Seconds)	17.225804
	Output image	
	Diagnosis	Consult Doctor Immediately Hair Line Crack (Normal Treatment, Take Rest and Don't Move Fractured Part)

6.2.3 Impacted Fracture

Table 6. 9 Impacted Fracture-1

Image Name	Description	Output
IF1.jpg	Input Image	
	Time Elapsed (in Seconds)	8.650212
	Output image	
	Diagnosis	Hair Line Crack (Normal Treatment, Take Rest and Don't Move Fractured Part) Minor Crack (Plaster Cast, Traction)

Table 6. 10 Impacted Fracture-2

Image Name	Description	Output
IF2.jpg	Input Image	
	Time Elapsed (in Seconds)	12.845981

	Output image	
	Diagnosis	Minor Crack (Plaster Cast, Traction)

Table 6. 11 Impacted Fracture-3

Image Name	**Description**	**Output**
IF3.jpg	**Input Image**	
	Time Elapsed (in Seconds)	15.676810
	Output image	
	Diagnosis	Consult Doctor Immediately.

Table 6. 12 Impacted Fracture-4

Image Name	Description	Output
IF4.jpg	**Input Image**	
	Time Elapsed (in Seconds)	16.276849
	Output image	
	Diagnosis	Consult Doctor Immediately.

6.2.4 Oblique Fracture

Table 6. 13 Oblique Fracture-1

Image Name	Description	Output
Ob1.jpg	Input Image	
	Time Elapsed (in Seconds)	6.665249
	Output image	
	Diagnosis	Consult Doctor Immediately

Table 6. 14 Oblique Fracture-2

Image Name	Description	Output
OB2.jpg	Input Image	
	Time Elapsed (in Seconds)	4.864156

	Output image	
	Diagnosis	Minor Crack (Plaster Cast, Traction)

Table 6. 15 Oblique Fracture-3

Image Name	**Description**	**Output**
OB3.jpg	**Input Image**	
	Time Elapsed (in Seconds)	3.094418
	Output image	
	Diagnosis	Hair Line Crack (Normal Treatment, Take Rest and Don't Move Fractured Part)

Table 6. 16 Oblique Fracture-4

Image Name	Description	Output
OB4.jpg	**Input Image**	
	Time Elapsed (in Seconds)	28.774336
	Output image	
	Diagnosis	Minor Crack (Plaster Cast, Traction)

6.2.5 Spiral Fractures

Table 6. 17 Spiral Fracture-1

Image Name	Description	Output
SF1.jpg	Input Image	
	Time Elapsed (in Seconds)	27.807226
	Output image	
	Diagnosis	Major Crack/Supracondylar fracture (External Fixation (Emergency)) False Detection

Table 6. 18 Spiral Fracture-2

Image Name	Description	Output
SF2.jpg	Input Image	
	Time Elapsed (in Seconds)	36.260223

	Output image	
	Diagnosis	Hair Line Crack (Normal Treatment, Take Rest and Don't Move Fractured Part) Minor Crack (Plaster Cast, Traction) Major Crack/Supracondylar fracture (External Fixation (Emergency))

Table 6. 19 Spiral Fracture-3

Image Name	**Description**	**Output**
SF3.jpg	**Input Image**	
	Time Elapsed (in Seconds)	619.847635
	Output image	
	Diagnosis	Consult Doctor Immediately Hair Line Crack (Normal Treatment, Take Rest and Don't Move Fractured Part) Minor Crack (Plaster Cast, Traction)

Table 6. 20 Spiral Fracture-4

Image Name	Description	Output
SF4.jpg	**Input Image**	
	Time Elapsed (in Seconds)	3.659930
	Output image	
	Diagnosis	Hair Line Crack (Normal Treatment, Take Rest and Don't Move Fractured Part)

6.2.6 Supra Condylar Fracture

Table 6. 21 Supra Condylar Fracture-1

Image Name	Description	Output
SC1.jpg	**Input Image**	
	Time Elapsed (in Seconds)	22.509672
	Output image	
	Diagnosis	Major Crack/Supracondylar fracture (External Fixation (Emergency)) Consult Doctor Immediately

Table 6. 22 Supra Condylar Fracture-2

Image Name	Description	Output
SC2.jpg	**Input Image**	
	Time Elapsed (in Seconds)	90.067583

	Output image	
	Diagnosis	Major Crack/Supracondylar fracture (External Fixation (Emergency)) Hair Line Crack (Normal Treatment, Take Rest and Don't Move Fractured Part)

Table 6. 23 Supra Condylar Fracture-3

Image Name	**Description**	**Output**
SC3.jpg	**Input Image**	
	Time Elapsed (in Seconds)	197.308952
	Output image	
	Diagnosis	Minor Crack (Plaster Cast, Traction) Major Crack/Supracondylar fracture (External Fixation (Emergency))

6.2.7 Transverse Fracture

Table 6. 24 Transverse Fracture-1

Image Name	Description	Output
TF1.jpg	Input Image	
	Time Elapsed (in Seconds)	18.527038
	Output image	
	Diagnosis	Major Crack (External Fixation (Emergency))

Table 6. 25 Transverse Fracture-2

Image Name	Description	Output
TF2.jpg	Input Image	
	Time Elapsed (in Seconds)	19.731682

	Output image	
	Diagnosis	Major Crack (External Fixation (Emergency))

Table 6. 26 Transverse Fracture-3

Image Name	**Description**	**Output**
TF3.jpg	**Input Image**	
	Time Elapsed (in Seconds)	9.122248
	Output image	
	Diagnosis	NIL

Table 6. 27 Transverse Fracture-4

Image Name	Description	Output
TF4.jpg	**Input Image**	
	Time Elapsed (in Seconds)	83.899059
	Output image	
	Diagnosis	Hair Line Crack (Normal Treatment, Take Rest and Don't Move Fractured Part) Crack/Supracondylar fracture (External Fixation (Emergency))

6.2.8 Avulsion Fracture;

Table 6. 28 Avulsion Fracture-1

Image Name	Description	Output
AF1.jpg	Input Image	
	Time Elapsed (in Seconds)	3.526332
	Output image	
	Diagnosis	Consult Doctor Immediately

Table 6. 29 Avulsion Fracture-2

Image Name	Description	Output
AF2.jpg	Input Image	
	Time Elapsed (in Seconds)	15.863343
	Output image	
	Diagnosis	Consult Doctor Immediately

Table 6. 30 Avulsion Fracture-3

Image Name	Description	Output
AF3.jpg	**Input Image**	
	Time Elapsed (in Seconds)	2.052098
	Output image	
	Diagnosis	Consult Doctor Immediately

6.2.9 Non Fracture

Table 6. 31 Non Fracture-1

Image Name	Description	Output
NF1.jpg	Input Image	
	Time Elapsed (in Seconds)	9.183006
	Output image	
	Diagnosis	True Detection

Table 6. 32 Non Fracture-2

Image Name	Description	Output
NF2.jpg	Input Image	
	Time Elapsed (in Seconds)	1.584016
	Output image	
	Diagnosis	True Detection

Table 6. 33 Non-Fracture-3

Image Name	Description	Output
NF3.jpg	Input Image	
	Time Elapsed (in Seconds)	3.943880
	Output image	
	Diagnosis	True Detection

Table 6. 34 Non Fracture-4

Image Name	Description	Output
NF4.jpg	Input Image	
	Time Elapsed (in Seconds)	3.536621
	Output image	
	Diagnosis	True Detection

Table 6. 35 Non Fracture-5

Image Name	Description	Output
NF5.jpg	**Input Image**	
	Time Elapsed (in Seconds)	10.445978
	Output image	
	Diagnosis	True Detection

Table 6. 36 Non Fracture-6

Image Name	Description	Output
NF6.jpg	**Input Image**	
	Time Elapsed (in Seconds)	57.295537
	Output image	
	Diagnosis	False Detection

Table 6. 37 Non Fracture-7

Image Name	Description	Output
NF7.jpg	**Input Image**	
	Time Elapsed (in Seconds)	5.687485
	Output image	
	Diagnosis	True Detection

6.3 Final Result

Recall (also known as sensitivity) is the fraction of relevant instances that have been retrieved over total relevant instances in the image.

$$\boldsymbol{Recall} = \frac{Number\ of\ Resultant\ image\ from\ Fracture\ Type}{Total\ Number\ of\ Image\ from\ Fracture\ Type}$$

Table 6. 38 Result Table

Fracture Image Type	Total Images	Correctly Detected	Not Correctly Detected	Recall
Compound	10	7	3	7/10 = 70
Comminuted	10	10	0	10/10 = 100
Impacted	10	10	0	10/10 = 100
Oblique	10	8	2	8/10 = 80
Spiral	10	10	3	7/10 = 70
Supracondylar	10	10	0	10/10 = 100
Transverse	10	5	5	5/10 = 50
Avulsion	10	10	0	10/10 = 100
Non-Fracture	10	8	2	8/10 = 80
TOTAL	90	**SYSTEM PERFORMANCE**		**83.33333**

Table 6. 39 Average Time Taken for finding ROI

Fracture Image Type	Average Time Taken for finding ROI in seconds for 10 images of each type
Compound	27.2575
Comminuted	67.4405
Impacted	13.3625
Oblique	10.8495
Spiral	171.894
Supracondylar	142.494
Transverse	32.82
Avulsion	7.14726
Non-Fracture	11.21033

Table 6. 40 Percentile Performance of the System

Fracture Image Type	Percentile
Compound	12.50
Comminuted	62.50
Impacted	62.50
Oblique	37.50
Spiral	12.50
Supracondylar	62.50
Transverse	0.00
Avulsion	62.50
Non-Fracture	37.50

By result, we understood that accuracy of the proposed algorithm is 83%. From the total dataset of images, the obtained results show that the system gives recall of 100 to 62.5 percentile images. The system gives minimum recall of 50. The average time to find the ROI (bone breakage) from 10 images is computed. From the obtained results, we can display that proposed system is fairly accurate for automatic identification of the region of interest (bone breakage) in X-ray medical images. The system also annotates the diagnosis

based on the size of the fracture and the course of treatment to be followed.

6.4 Discussion

A percentile [59] is a measure used in statistics indicating the value below which a given percentage of observations in a group of observations fall. For example, the value of 0 percentile as in Table 6.40 for the transverse fracture type suggest that there is no other fracture type having less percentage than transverse fracture type i.e. 50% as in table 6.38. So we have achieved a minimum 50% of success ratio in all the cases and no type has less than 50% success ratio for our algorithm.

For many different types of fractures, we have run the application made from ROIMI algorithm that is proposed and we have found the satisfactory result. Results were promising in around 83% of the cases ROI that was detected was proper to identify the fracture in the bone. There were some other areas also found out but the crack was exactly found out along with the suggestion of the diagnosis. In case of utmost emergency, our proposed algorithm can save the life of a patient by taking a proper decision at right time.

Because in case of closed fracture it is observed that if it is not a simple fracture then there are chances of bone coming out of the body and then many complications can arise.

Before starting of development of algorithm doctors were consulted and according to them mainly cracks in the human body were categorized in the hair-line crack, minor crack, and major crack. Also from the various literature, we have found that there were problems in this domain and research is going on to find the exact bone part in different areas of human organs. So we concentrated on long bone parts and then the results obtained were verified with the doctor and he was happy with the result that was given by the system developed from our algorithm.

Also, X-Rays images were acquired from various sources and tested for the performance of the system. We have seen that X-Ray obtained from different locations were having a different type of noise associated with it or contrast. So the pre-processing step was necessary to be performed. Also, results were tested when there was no fracture in the bone and it gave us the satisfactory result.

CHAPTER 7

Conclusion and Future Work

7.1 Conclusion

This chapter gives a short discussion on the achievements of this work, concluding and giving suggestions for further work to be undertaken.

The work presented in this thesis addresses the need of the hour for computer-assisted identification and diagnosis of fractures in the bone X-ray images and the fully automated algorithm is developed for the same and tested. The hierarchical algorithm loads the X-ray image of the bone. The preprocessing steps remove noise and the unwanted background from the image for better segmentation results. The exact bone structures are extracted from the image using segmentation based on Active contours without edges. Novel ROIMI approach is developed for identification of potential fractures. The identified fractures are then classified as per their size and the diagnosis is annotated on the final restored original image along with potential fractures highlighted in red color.

The results obtained so far are promising and indicates potential clinical application. As the proposed work is fully automated to identify fractures and provide preliminary diagnosis, it can prove to be resourceful and fundamental in saving any patient's life in any emergency

situations arise in the absence of the medical practitioner.

The main purpose of developing the system to provide faster and accurate diagnostic decision support as a step towards providing better healthcare and serve the humankind.

7.2 Future Work:

The work presented in this thesis represents the initial efforts in developing a capable and intuitive algorithm for segmentation and identification of bone fractures and providing a diagnosis as a decision support for a preliminary course of action.

Our experimental results on images of different fracture types encourage further research along with many different directions which will tend to improve and make the method more efficient. The algorithm was tested with a dataset of images of different types of fractures. The results obtained show that the algorithm is able to identify 8 different fracture types, but poses a limitation by not being able to identify a vertical type of fracture. This generates a possibility of enhancement and future work. Time efficiency can be improved to fasten the process of determining the fracture. An application can be developed to merge the algorithm with the hardware like Plate Scanner Machine.

List of References

List of References

[1] "http://indiatoday.intoday.in/," *http://indiatoday.intoday.in/*.

[2] S. Thammasitboon and W. B. Cutrer, "Diagnostic decision-making and strategies to improve diagnosis," *Curr. Probl. Pediatr. Adolesc. Health Care*, vol. 43, no. 9, pp. 232–241, Oct. 2013.

[3] Arun Baran Singha Mahapatra., *Essentials of medical physiology. ISBN 81-86793-56-9*.

[4] P. Chakraborty; G. Chakraborty., *Practical Pathology. ISBN 81-7381-332-9.*

[5] Robbins and Cotran, *Review of Pathology. ISBN 0-7216-0194-4*.

[6] David Sutton, *Radiology and imaging for med. students (7th ed.). ISBN 81-7867-100-X.*

[7] "Automated medical image segmentation techniques Sharma N, Aggarwal LM - J Med Phys." [Online]. Available: http://www.jmp.org.in/article.asp?issn=0971-6203;year=2010;volume=35;issue=1;spage=3;epage=14;aulast=Sharma.

[8] D. J. Withey and Z. J. Koles, "Medical Image Segmentation: Methods and Software," in *2007 Joint Meeting of the 6th International Symposium on Noninvasive Functional Source Imaging of the Brain and Heart and the International Conference on Functional Biomedical Imaging*, 2007, pp. 140–143.

[9] N. Otsu, "A Threshold Selection Method from Gray-Level Histograms," *IEEE Trans. Syst. Man Cybern.*, vol. 9, no. 1, pp. 62–66, Jan. 1979.

[10] T. McInerney and D. Terzopoulos, "Deformable models in medical image analysis," in *Mathematical methods in biomedical image analysis, 1996., Proceedings of the workshop on*, 1996, pp. 171–180.

[11] T. F. Cootes and C. J. Taylor, "Statistical models of appearance for medical image analysis and computer vision," in *Medical Imaging 2001*, 2001, pp. 236–248.

[12] N. Umadevi and S. N. Geethalakshmi, "Multiple classification systems for fracture detection in human bone x-ray images," in *2012 Third International Conference on Computing Communication Networking Technologies (ICCCNT)*, 2012, pp. 1–8.

[13] G. K. Manos, A. Y. Cairns, I. W. Rickets, and D. Sinclair, "Segmenting radiographs of the hand and wrist," *Comput. Methods Programs Biomed.*, vol. 43, no. 3, pp. 227–237, Jun. 1994.

[14] N. F. Vittitoe, R. Vargas-Voracek, and C. F. Floyd, "Identification of lung regions

in chest radiographs using Markov random field modeling," *Med. Phys.*, vol. 25, no. 6, pp. 976–985, Jun. 1998.

[15] "Lung segmentation in digital radiographs | SpringerLink." [Online]. Available: https://link.springer.com/article/10.1007/BF03168427.

[16] "A fully automated algorithm for the segmentation of lung fields on digital chest radiographic images. - PubMed - NCBI." [Online]. Available: https://www.ncbi.nlm.nih.gov/pubmed/7565349.

[17] H. C. Chen, C. H. Wu, C. J. Lin, Y. H. Liu, and Y. N. Sun, "Automated segmentation for patella from lateral knee X-ray images," *Conf. Proc. Annu. Int. Conf. IEEE Eng. Med. Biol. Soc. IEEE Eng. Med. Biol. Soc. Annu. Conf.*, vol. 2009, pp. 3553–3556, 2009.

[18] M. G. Roberts, T. Oh, E. M. B. Pacheco, R. Mohankumar, T. F. Cootes, and J. E. Adams, "Semi-automatic determination of detailed vertebral shape from lumbar radiographs using active appearance models," *Osteoporos. Int. J. Establ. Result Coop. Eur. Found. Osteoporos. Natl. Osteoporos. Found. USA*, vol. 23, no. 2, pp. 655–664, Feb. 2012.

[19] T. Xu, M. Mandal, R. Long, and A. Basu, "Gradient vector flow based active shape model for lung field segmentation in chest radiographs," in *2009 Annual International Conference of the IEEE Engineering in Medicine and Biology Society*, 2009, pp. 3561–3564.

[20] B. van Ginneken, M. B. Stegmann, and M. Loog, "Segmentation of anatomical structures in chest radiographs using supervised methods: a comparative study on a public database," *Med. Image Anal.*, vol. 10, no. 1, pp. 19–40, Feb. 2006.

[21] N. Boukala, E. Favier, B. Laget, and P. Radeva, "Active shape model-based segmentation of bone structures in hip radiographs," in *2004 IEEE International Conference on Industrial Technology, 2004. IEEE ICIT '04*, 2004, vol. 3, p. 1682–1687 Vol. 3.

[22] D. L. Pham, C. Xu, and J. L. Prince, "Current methods in medical image segmentation 1," *Annu. Rev. Biomed. Eng.*, vol. 2, no. 1, pp. 315–337, 2000.

[23] A. Aprovitola and L. Gallo, "Knee bone segmentation from MRI: A classification and literature review," *Biocybern. Biomed. Eng.*, vol. 36, no. 2, pp. 437–449, 2016.

[24] T. Kapur, P. Beardsley, S. Gibson, W. Grimson, and W. Wells, "Model-based segmentation of clinical knee MRI," in *Proc. IEEE Int'l Workshop on Model-Based 3D Image Analysis*, 1998, pp. 97–106.

[25] Y. Sun, E. C. Teo, and Q. H. Zhang, "Discussions of Knee joint segmentation," in *Biomedical and Pharmaceutical Engineering, 2006. ICBPE 2006. International Conference on*, 2006.

[26] C. Xu and J. L. Prince, "Snakes, shapes, and gradient vector flow," *IEEE Trans. Image Process.*, vol. 7, no. 3, pp. 359–369, Mar. 1998.

[27] B. Fischer and J. Modersitzki, "A unified approach to fast image registration and a new curvature based registration technique," *Linear Algebra Its Appl.*, vol. 380, pp. 107–124, Mar. 2004.

[28] H. Arabi and H. Zaidi, "Comparison of atlas-based techniques for whole-body bone segmentation," *Med. Image Anal.*, vol. 36, pp. 98–112, Feb. 2017.

[29] H. Arabi and H. Zaidi, "Comparison of atlas-based bone segmentation methods in whole-body PET/MRI," in *Nuclear Science Symposium and Medical Imaging Conference (NSS/MIC), 2014 IEEE*, 2014, pp. 1–4.

[30] F. Ding, W. K. Leow, and T. S. Howe, "Automatic Segmentation of Femur Bones in Anterior-Posterior Pelvis X-Ray Images," in *Computer Analysis of Images and Patterns*, 2007, pp. 205–212.

[31] B. Shinde, D. Mhaske, and A. R. Dani, "Study of Noise Detection and Noise Removal Techniques in Medical Images," *Int. J. Image Graph. Signal Process.*, vol. 4, no. 2, pp. 51–60, Mar. 2012.

[32] S. Patil and V. R. Udupi, "Preprocessing to be considered for MR and CT images containing tumors," *IOSR J. Electr. Electron. Eng.*, vol. 1, no. 4, pp. 54–57, 2012.

[33] Gursharan Kaur,Rakesh Kumar, Kamaljeet Kainth, "A Review Paper on Different Noise Types and Digital Image Processing," *International Journal of Advanced Research in Computer Science and Software Engineering*, vol. 6, no. 6, Jun. 2016.

[34] Kaur Rupinderpal, Kaur Rajneet, "Survey of De-noising Methods Using Filters and Fast Wavelet Transform," *International Journal of Advanced Research in Computer Science and Software Engineering,* vol. 3, no. 2, pp. 134–136, Feb. 2013.

[35] Sezal Khera, Sheenam Malhotra, "Survey on Medical Image De noising Using various Filters and Wavelet Transform," *International Journal of Advanced Research in Computer Science and Software Engineering*, vol. 4, no. 4, Apr. 2014.

[36] S. Mallat and S. Zhong, "Characterization of signals from multiscale edges," *IEEE Trans. Pattern Anal. Mach. Intell.*, vol. 14, no. 7, pp. 710–732, Jul. 1992.

[37] L. Kleeman, "Understanding and applying Kalman filtering," in *Proceedings of the Second Workshop on Perceptive Systems, Curtin University of Technology, Perth*

Western Australia (25-26 January 1996), 1996.

[38] S. E. Umbaugh, *Digital Image Processing and Analysis: Human and Computer Vision Applications with CVIPtools, Second Edition*. CRC Press, 2010.

[39] P. Sharma, G. Singh, and A. Kaur, "Different techniques of edge detection in digital image processing," *Int. J. Eng. Res. Appl. IJERA*, vol. 3, no. 3, pp. 458–461, 2013.

[40] Anil K. Jain, *Fundamentals of Digital Image Processing*. 1989.

[41] R. C. Gonzalez, *Digital Image Processing*. Pearson Education India, 2009.

[42] R. Muthukrishnan and M. Radha, "Edge Detection Techniques For Image Segmentation," *Int. J. Comput. Sci. Inf. Technol.*, vol. 3, no. 6, pp. 259–267, Dec. 2011.

[43] J. Canny, "A Computational Approach to Edge Detection," *IEEE Trans. Pattern Anal. Mach. Intell.*, vol. PAMI-8, no. 6, pp. 679–698, Nov. 1986.

[44] R. Shah and P. Sharma, "Performance analysis of region of interest based compression method for medical images," in *Advanced Computing & Communication Technologies (ACCT), 2014 Fourth International Conference on*, 2014, pp. 53–58.

[45] H. C. Kang, Y.-G. Shin, and J. Lee, "Automatic segmentation of skin and bone in CT images using iterative thresholding and morphological image processing," in *Consumer Electronics (ISCE 2014), The 18th IEEE International Symposium on*, 2014, pp. 1–2.

[46] D. Peng, B. Merriman, S. Osher, H. Zhao, and M. Kang, "A PDE-Based Fast Local Level Set Method," *J. Comput. Phys.*, vol. 155, no. 2, pp. 410–438, Nov. 1999.

[47] T. F. Chan and L. A. Vese, "Active contours without edges," *IEEE Trans. Image Process.*, vol. 10, no. 2, pp. 266–277, 2001.

[48] Daniel J. Power, *Decision Support Systems: Concepts and Resources for Managers*. 2002.

[49] "Medical Decision Support Systems and Knowledge Sharing Standards." [Online]. Available: http://what-when-how.com/medical-informatics/medical-decision-support-systems-and-knowledge-sharing-standards/.

[50] V. K. Omachonu and N. G. Einspruch, "Innovation in healthcare delivery systems: a conceptual framework," *Innov. J. Public Sect. Innov. J.*, vol. 15, no. 1, pp. 1–20, 2010.

[51] P. Croskerry and G. Nimmo, "Better clinical decision making and reducing diagnostic error," *J. R. Coll. Physicians Edinb.*, vol. 41, no. 2, pp. 155–162, Jun. 2011.

[52] “More on colors and grayscale.” [Online]. Available: https://www.johndcook.com/blog/2009/08/24/more-on-colors-and-grayscale/.

[53] “5.10. Desaturate.” [Online]. Available: https://docs.gimp.org/2.6/en/gimp-tool-desaturate.html.

[54] B. Rajitha and S. Agarwal, “An Iterative Thresholding Method for Epiphysis ROI Segmentation for Radiographic Images,” 2015, pp. 1–7.

[55] “Distance transform of binary image - MATLAB bwdist - MathWorks India.” [Online]. Available: http://in.mathworks.com/help/images/ref/bwdist.html.

[56] R. Malladi, J. A. Sethian, and B. C. Vemuri, “Shape modeling with front propagation: a level set approach,” *IEEE Trans. Pattern Anal. Mach. Intell.*, vol. 17, no. 2, pp. 158–175, Feb. 1995.

[57] “Multilevel image thresholds using Otsu’s method - MATLAB multithresh - MathWorks India.” [Online]. Available: https://in.mathworks.com/help/images/ref/multithresh.html.

[58] G. Gao, C. Wen, and H. Wang, “Fast and robust image segmentation with active contours and Student’s-t mixture model,” *Pattern Recognit.*, vol. 63, pp. 71–86, Mar. 2017.

[59] “Percentile,” *Wikipedia*. 15-Jun-2017.

List of Publications

Patent:

"Decision Support System for Automatic Identification of Region of Interest for Medical Images", Application Number 201721037688; Date of filing October 21, 2017; Date of publication November 10, 2017.

Book Chapters

1. R. Shah et al. "Bone Segmentation from X-ray images: Challenges and Techniques" Information Systems Design and Intelligent Applications: Proceedings of Fourth International Conference India 2017. Vol. 672. Bhateja, Vikrant and S. Das, Eds. Cham: Springer International Publishing, 2018, pp. 878-887.
2. R. Shah et al., "Comparative Performance Study of Various Content-Based Image Retrieval Methods," in Proceedings of First International Conference on Information and Communication Technology for Intelligent Systems: Volume 1, vol. 50, S. C. Satapathy and S. Das, Eds. Cham: Springer International Publishing, 2016, pp. 397–407.

International Conference

1. Shah, Rutvi, and Priyanka Sharma. "Bone Segmentation from X-Ray Images: Challenges and Techniques." Information Systems Design and Intelligent Applications. Springer, Singapore, 2018. 853-862.
2. Shah Rutvi, Shah Rushabh, Lavingiya Kruti, "GDLC: A Software Approach in Game Development," presented at the International Journal of Advance Research in Science and Engineering, Vol. No. 6 Issue No 06, June 2017.
3. R. Shah *et al.*, "Comparative Performance Study of Various Content-Based Image Retrieval Methods," in *Proceedings of First International Conference on Information and Communication Technology for Intelligent Systems: Volume 1*, vol. 50, S. C. Satapathy and S. Das, Eds. Cham: Springer International Publishing, 2016, pp. 397–407.

4. R. Shah, Prof. R Shah, Dr. Priyanka Sharma, “Survey of Region of Interest and its Applicative Utility in various areas of the medical field,” presented at the International Conference on Recent Trends in Engineering Science and Management, 2015.
5. Shah, Rushabh, Priyanka Sharma, and Rutvi Shah. "Performance analysis of region of interest based compression method for medical images." Advanced Computing & Communication Technologies (ACCT), 2014 Fourth International Conference on. IEEE, 2014. Received “BEST PAPER AWARD” for the paper.

National Conference

1. R. Shah, Prof. RR Shah, Dr. Priyanka Sharma, “Clinical Decision Support System: An Efficient Structure for providing High-Quality Patient Care,” presented at the National Conference On Emerging Trends in Information and Communication Technology 2013.

International Journal

1. R. Shah, Prof. R Shah, Dr. Priyanka Sharma, “Survey of Region of Interest and its Applicative Utility in various areas of the medical field,” Published at International Journal of Advanced Technology in Engineering and Science www.ijates.com, Volume No 3, Special Issue No 01, ISSN 2348-7550, March 2015.
2. Dr. Priyanka Sharma, R Shah, Prof. R Shah, “Implementation of E-learning Using Mobile Technology”, Published at International Journal of Information and Computing Technology, Volume 3, Issue No 1, ISSN 0976-5999, December 2013

MOOC Courses Done

1. Coursera Course on **“Fundamentals of Digital Image and Video Processing”** in 2016.

2. Coursera Course on **"Introduction to Programming with Matlab"** by Vanderbilt University in 2015.
3. Coursera Course on **"Image and Video Processing: From Mars to Hollywood with a stop at the Hospital"** by Duke University in 2014.

Achievements

- **Patent** filed for the research work done.
- Presented and Published 5 papers at International conferences and 1 at the National conference.
- Published 2 papers at International journals.
- Received "**Best Paper Award**" for the paper presented at IEEE international conference and published in IEEE Digital Explore.
- Two of the presented papers has been published as a book chapters in Springer books.
- The papers published in IEEE and Springer are listed in Google Scholar and Scopus.
- The presented papers have been cited by 13 authors on Google Scholar and by 3 authors on Scopus. The H index of citations is1.
- Successfully completed the course of "Image and Video Processing" from Coursera.org in collaboration with Duke University, North Carolina with distinction.
- Successfully completed the course of "Fundamentals of Digital Image and Video Processing" from Coursera.org with distinction.
- Successfully completed the course of "Image and Video Processing" from Coursera.org in collaboration with Duke University, North Carolina with distinction.